

A Last Interglacial record of environmental changes from the Sulmona Basin (central Italy)

Eleonora [Regattieri](#)^{1a, 2b, 3c, *}

regattieri@dst.unipi.it

Biagio [Giaccio](#)^{2d}

Sebastien [Nomade](#)^{4d}

Alexander [Francke](#)^{1a}

Hendrik [Vogel](#)^{5e}

Russell N. [Drysdale](#)^{6f, 7g}

Natale [Perchiazzi](#)^{9h}

Bernd [Wagner](#)^{1a}

Maurizio [Gemelli](#)^{9h}

Ilaria [Mazzini](#)^{2b}

Chiara [Boschi](#)^{3c}

Paolo [Galli](#)^{2b, 9i}

Edoardo [Peronace](#)^{2b}

^{1a}Institute of Geology and Mineralogy, University of Cologne, Zùlpicher Str. 49a, 50674 Cologne, Germany

^{2b}Istituto di Geologia Ambientale e Geingegneria, IGAG-CNR, Via Salaria km. 29.4, Monterotondo, Rome, Italy

^{3c}Istituto di Geoscienze e Georisorse, IGG-CNR, Via Moruzzi 1, 56126 Pisa, Italy

^{4d}Laboratoire des Sciences du Climat et de l'Environnement, IPSL, Laboratoire CEA/CNRS/UVSQ et Université de Paris-Saclay, Gif-Sur-Yvette, France

^{5e}Institute of Geological Sciences & Oeschger Centre for Climate Change Research, University of Bern, Switzerland

^{6f}School of Geography, University of Melbourne, Victoria 3010, Australia

^{7g}EDYTEM, UMR CNRS 5204, Université de Savoie-Mont Blanc, 73376 Le Bourget du Lac-Cedex, France

^{9h}Dipartimento di Scienze della Terra, University of Pisa, Via S. Maria 53, 56126 Pisa, Italy

⁹ⁱDipartimento di Protezione Civile, Via Vitorchiano 4, 00189 Rome, Italy

*Corresponding author at: Istituto di Geoscienze e Georisorse, IGG-CNR, Via Moruzzi 1, 56126 Pisa, Italy.

Abstract

Here we present a multiproxy record ($\delta^{13}\text{C}$, $\delta^{18}\text{O}$, major and minor element composition, mineralogy, and low-resolution biogenic silica content) from a lacustrine succession in the Sulmona Basin, central

Italy. Based on previous tephrochronological constraints and a new $^{40}\text{Ar}/^{39}\text{Ar}$ dating of a tephra matching the widespread X-6 tephra, the record spans the ca. 129–92 ka period and documents at sub-orbital scale the climatic and environmental changes over the Last Interglacial and its transition to the Last Glacial period. The $\delta^{18}\text{O}$ composition is interpreted as a proxy for the amount and seasonality of local precipitation, whereas variations in elemental and mineralogical composition are inferred to reflect climatic-driven changes in clastic sediment input. The observed variations are consistent among the different proxies, and indicate that periods of reduced precipitation were marked by enhanced catchment erosion, probably due to a reduction in vegetation cover. The first part of the Last Interglacial shows the most negative $\delta^{18}\text{O}$ values. Comparison with pollen records from the Mediterranean suggests a greater seasonality of the precipitation at this time. At millennial-to-centennial time scales, comparison of the Sulmona record with speleothem $\delta^{18}\text{O}$ records from central Italy highlights a highly coherent pattern of hydrological evolution, with enhanced variability and similar events of reduced precipitation consistently recorded by each isotope record. The observed intra-interglacial variability can potentially be linked, within the uncertainties associated with each age model, to similar variations observed in sea-surface temperature records from the Mediterranean and the North Atlantic, suggesting a link between Mediterranean hydrology and North Atlantic temperature and circulation patterns that persists during periods of low ice volume.

Keywords: Paleoclimate; [sStable isotopes](#); [Llacustrine succession](#); [Ttephrochronology](#)

1.1 Introduction

The climate of the Last Interglacial (LIG), roughly corresponding to marine isotope stage (MIS) 5e and the Eemian interglacial in the European pollen stratigraphy (Govin et al., 2015 and references therein), has many features in common with model projections of future climate, because during this period much of the Earth experienced a climate warmer than present (e.g. Kukla et al., 2002). Although orbital parameters for MIS5e are quite different from that of the Holocene (e.g. Berger and Loutre, 1991), the LIG is a potential analog for projected future global warming and is thus an interesting study case for evaluating the climate and environmental responses during periods characterized by an excess of warmth. From this perspective, of particular interest are intra-interglacial millennial-scale climate changes. Evidence of abrupt climatic variations are well documented in several LIG records from North Atlantic marine sediments and Greenland ice (e.g. Oppo et al., 2001, 2006; Galaasen et al., 2014; Pol et al., 2014) and some seem to have propagated into the Mediterranean basin (Sánchez-Goñi et al., 1999; Martrat et al., 2004, 2014; Sprovieri et al., 2006; Kandiano et al., 2014). Potential expressions of this oceanic driven instability have also been recognized in central Europe (e.g. Sirocko et al., 2005; Seelos and Sirocko, 2007; Seelos et al., 2009), as well as in the Mediterranean region (e.g. Tzedakis et al., 2003; Brauer et al., 2007; Drysdale et al., 2007; Couchoud et al., 2009; Milner et al., 2013, 2016; Regattieri et al., 2014a, 2016a; Vogel et al., 2010; Lézine et al., 2010; Zanchetta et al., 2016a, 2016b). However, the effects of such changes on climate and ecosystems of the European continent are still poorly known and understood (Galaasen et al., 2014; Govin et al., 2015). Identification, correlation and evaluation of the climatic expressions of LIG millennial-scale variability outside the North Atlantic region remain unclear or largely based on postulated temporal phase relations. Addressing these issues requires the compilation of regionally representative, high-resolution and independently dated paleoclimatic records. Lacustrine successions deposited in tectonic basins of the Apennines are capable of fulfilling these requirements (Giaccio et al., 2015a, 2015b; Regattieri et al., 2015, 2016b; Russo-Ermolli et al., 2010) due to the high sensitivity of the local sediment properties, and particularly of the oxygen stable isotope composition of authigenic carbonates ($\delta^{18}\text{O}$), to hydrological and environmental changes. Moreover, these archives offer the possibility to develop independent age models based on the $^{40}\text{Ar}/^{39}\text{Ar}$ geochronometer (C) that can be directly or indirectly applied to the volcanic ash layers (tephra). These tephra layers, deriving from the intense activity of Quaternary peri-Tyrrhenian explosive volcanism, are systematically found in the lacustrine sediments of the Apennine intermountain basins (e.g. Giaccio et al., 2012; Petrosino et al., 2014; Giaccio et al., 2017 (please add this reference, which has also been added in the references list)).

Of the central Italian continental basins, Sulmona has already been recognized as a promising archive. The sedimentary record is underpinned by a robust tephrochronological framework (Giaccio et al., 2012, 2013a, 2013b), and provides important insights into climate and environmental evolution of the central Mediterranean and the linkages with extra-regional climate variability (Giaccio et al., 2015a; Regattieri et al., 2015, 2016b). In particular, the stable isotope profiles ($\delta^{18}\text{O}$ and $\delta^{13}\text{C}$), CaCO_3 content and tephrostratigraphy of the Popoli section (POP hereafter), documenting Early Last Glacial climate fluctuations (from ca. 115 to ca. 90 ka), highlight strong Mediterranean–North Atlantic climate teleconnections as well as the influence of low-latitude circulation patterns (Regattieri et al., 2015). In order to explore the environmental-hydrological changes over the entire early-to-middle MIS 5 (MIS 5e to MIS 5c, ca. 129–92 ka), and in particular the intra-LIG millennial scale variability, in this study we extended through a multiproxy approach ($\delta^{18}\text{O}$ and $\delta^{13}\text{C}$ analysis, CaCO_3 content, biogenic silica content, XRF major and minor element composition, XRD-based bulk mineralogy and $^{40}\text{Ar}/^{39}\text{Ar}$ geochronology) the investigation of the POP section back to ca.129 ka. The results provide a longer and richer multi-proxy record, which allows a detailed reconstruction of local environmental change and give insights on potential relations with the extra-regional millennial-scale variability during the full LIG and at the LIG/Last Glacial transition.

2.2 Study site

2.1.2.1 Geological and stratigraphic setting

An up-dating stratigraphic framework of the Sulmona Basin (Fig. 1 (please find attached a corrected version of Figure 1, there was a typo in the previous one.)) is provided in Giaccio et al. (2009 with amendments in Giaccio et al., 2013a; 2012), Galli et al. (2015) and Regattieri et al. (2015, 2016b), to which the reader is referred for integrating the information summarized here. The Sulmona Basin (Fig. 1) is a block-faulted intermontane depression which accumulated lacustrine sediments discontinuously during the Quaternary (e.g. Cavinato et al., 1994; Cavinato and Miccadei, 1995, 2000; Miccadei et al., 1998; Giaccio et al., 2012, 2013a). The exposed Pleistocene succession in the Sulmona basin is composed of three main unconformity-bound, alluvial-fluvial-lacustrine units (SUL 6, SUL 5 and SUL 4-3), chronologically constrained by magnetostratigraphy and tephrochronology (Giaccio et al., 2012, 2013a, 2013b, 2015a; Sagnotti et al., 2014, 2016). The interval investigated here (POP section) corresponds to the lowermost part of the SUL 4-3 unit (ca. 110–14 ka, Fig. 1). The outcropping portion of the POP section (~ 19 m from the top of the lacustrine deposits; Fig. 1) has been described by Giaccio et al. (2012), with particular attention to its tephrostratigraphy, and by Regattieri et al. (2015), who presented the stable isotope results ($\delta^{13}\text{C}$ and $\delta^{18}\text{O}$) from the lacustrine carbonates and extended the tephrostratigraphic investigation down to ~ 27 m of the outcrop depth (Fig. 1) by means of a trench and a borehole (Fig. 1).

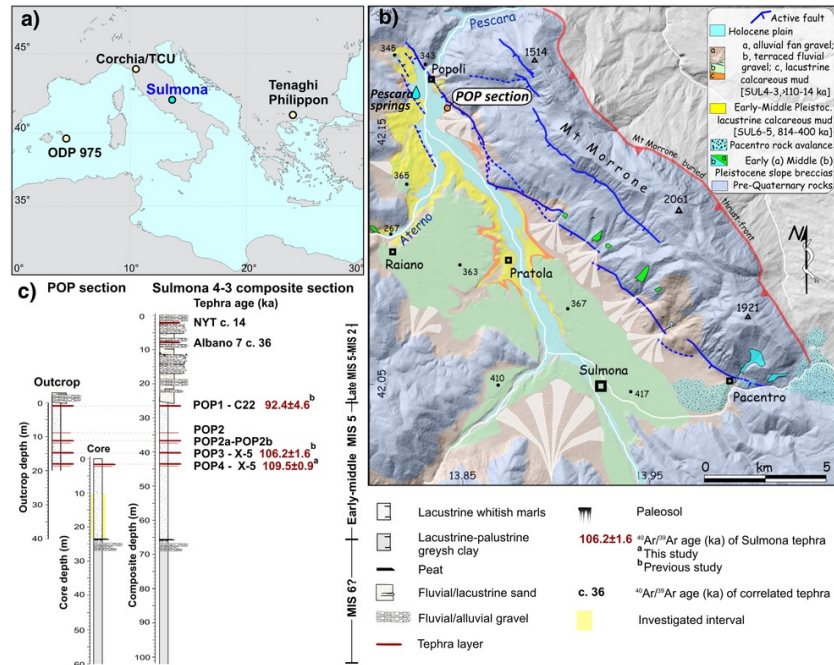


Fig. 1 Reference maps of the investigated sedimentary succession. (a) Location of the Sulmona Basin and other sites mentioned in the text; (b) simplified geological map of Sulmona Basin with the location of the POP section investigated here (from Galli et al., 2015). (c) Lithostratigraphy and tephrochronology of the POP section and of the whole composite section of SUL4-3 unit; NYT: Neapolitan Yellow Tuff.

alt-text: Fig. 1

Six tephras were previously recognized in the POP section, named from top to the base POP1, POP2, POP2a, POP2b, POP3 and POP4 (Figs. 1 and 2). Descriptions, tephrostratigraphic correlations with other archives and ages for these tephras have been provided by Giaccio et al. (2012) and Regattieri et al. (2015) and are summarized in Table 1. Here, we present a new $^{40}\text{Ar}/^{39}\text{Ar}$ age for tephra POP4, which chemically matches the X-6 tephra (Regattieri et al., 2015) of the marine tephrostratigraphic schemes of Keller et al. (1978). This tephra shows a large dispersal area covering the central Mediterranean and the Balkans (Bourne et al., 2015; Donato et al., 2016; Insinga et al., 2014, Iorio et al., 2014; Leicher et al., 2016; Lézine et al., 2010; Petrosino et al., 2016; Sulpizio et al., 2010; Vogel et al., 2010).

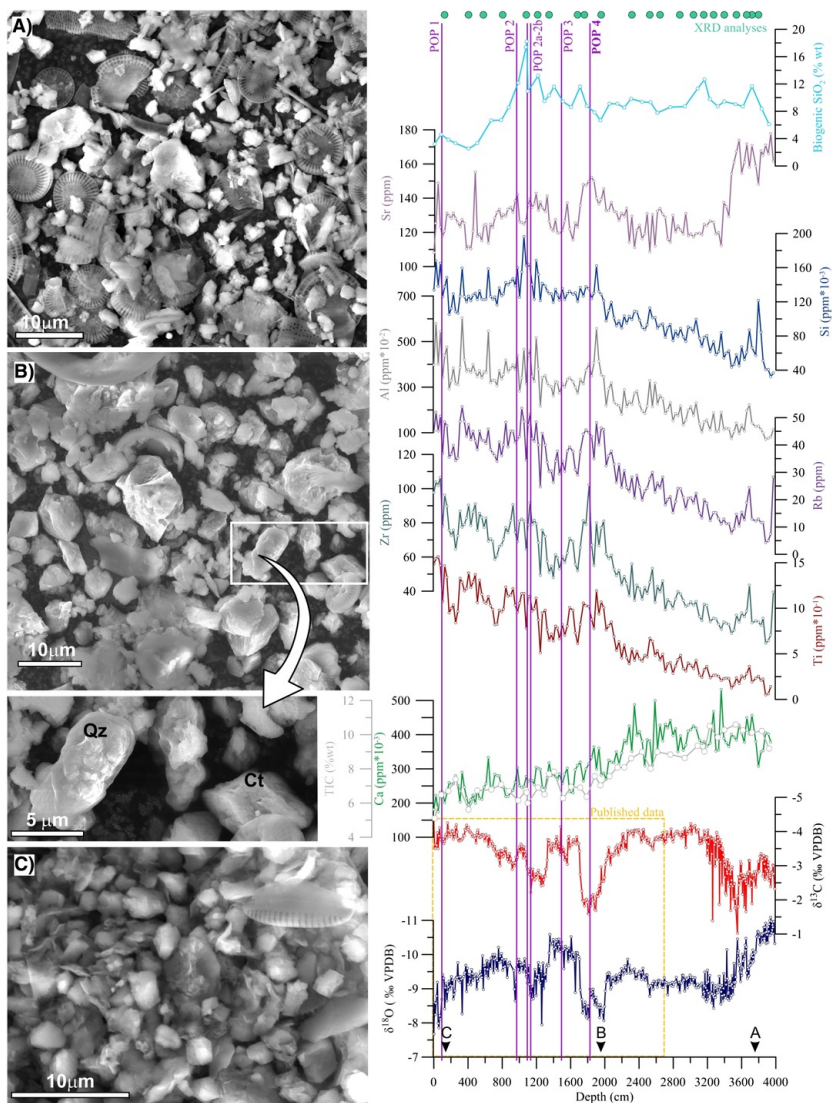


Fig. 2 Micro-features and proxy data from the lacustrine sediments of POP succession. Right panel: Field Emission Scanning Electron Microscopy (FESEM) images of selected samples. The depths of the three samples A, B and C ~~is~~ **are** indicated by the corresponding letters on the depth scale of the left panel. Left panel: POP stable isotope, trace element, mineralogical and organic carbon results plotted vs. depth. From bottom: $\delta^{18}\text{O}$ and $\delta^{13}\text{C}$ (within yellow box stable isotope data already published by [Regattieri et al., 2015](#)); Ca and Total Inorganic Carbon (TIC), Ti, Zr, Rb, Al, Si, Sr (XRF data converted to ppm), biogenic silica (% total weight). Purple lines represent tephra layers. Position of XRD analyses (green dots on top) and of FESEM pictures (letters) is also shown. [\(For interpretation of the references to colour in this figure legend, the reader is referred to the web version of this article.\)](#)

alt-text: Fig. 2

Table 1 Tephra ages and correlations between POP, Monticchio ([Brauer et al., 2007](#); [Wulf et al., 2012](#)) and Mediterranean marine ([Keller et al., 1978](#); [Paterne et al., 2008](#)) tephra as proposed by [Giaccio et al. \(2012\)](#) and [Regattieri et al. \(2015\)](#). The resulting modelled tephra ages obtained by the Clam algorithm ([Blaauw, 2010](#)) are also shown.

alt-text: Table 1

Sulmona POP section			Monticchio record	Marine record	POP age model (ka) $\pm 2\sigma$	
Tephra	Depth (m)	$^{40}\text{Ar}/^{39}\text{Ar}$ age (ka) $\pm 2\sigma$ uncertainty	Tephra	Tephra	Initial age	Modelled age
POP1	0.935	92.4 \pm 4.6 ^a	TM-23-11	C-22	92.4 \pm 4.6 ^a	93.4 \pm 4.5
POP2	9.690		TM-24-a		101.8 \pm 5.0 ^b	101.8 \pm 1.8
POP2a	10.935		TM-24-b		102.8 \pm 5.1 ^b	101.4 \pm 1.5
POP2b	11.335		TM-24-3b	C-26	104.0 \pm 1.0 ^b	103.3 \pm 1.4
POP3	14.935	106.2 \pm 1.3 ^a	TM-25	C-27/X-5	106.2 \pm 1.3 ^a	106.6 \pm 0.9
POP4	18.260	109.5 \pm 0.9^c	TM-27	C-31/X-6	109.5 \pm 0.9^c	109.6 \pm 1.4

Tephra ages from:

^a [Giaccio et al. \(2012\)](#).

^b [Wulf et al. \(2012\)](#).

^c The present study.

2.2.2.2 Climatic and hydrological settings

The Sulmona Basin is located in the central Apennines ([Fig. 1](#)) at a mean elevation of \sim 400 m a.s.l. The current mean annual temperature is 13.7 °C and the mean annual rainfall is 870 mm (data from the Sulmona meteorological station). About 60% of the region's precipitation has a North Atlantic origin, especially during winter, whereas the other 40% is mainly sourced from the western Mediterranean ([Bard et al., 2002](#)). The present hydrology of the basin is dominated by large perennial springs fed by the extensive karst systems hosted in the mountains surrounding the basin, where precipitation reaches values of about 1200 mm/year at the summits. These springs are mainly fed by recharge at 1200–1500 m a.s.l. with minor input from higher altitudes (up to 2900 m a.s.l., [Barbieri et al., 2005](#); [Desiderio et al., 2005a, 2005b](#)). Because they are recharged at higher altitude, the springs have a $\delta^{18}\text{O}$ composition lower than local precipitation (which is \sim 7.13‰, data from L'Aquila station, [Longinelli and Selmo, 2003](#)). Discharge is higher during early spring due to snowmelt, lowering further the average $\delta^{18}\text{O}$ isotopic values of water recharging the basin ([Falcone et al., 2008](#)). Waters also have a higher $\delta^{13}\text{C}$ of dissolved inorganic carbon (DIC) compared with that of the more superficial springs due to longer water residence times and rock-water interactions within the karst ([Falcone et al., 2008](#)). These springs represented the main source also for the studied paleo-lake and, likely, hydrological conditions of the high-altitude catchment area dominated its recharge, both during drier and wetter periods ([Regattieri et al., 2015, 2016b](#); [Giaccio et al., 2015a](#)).

3.3 Material and Methods

3.1.3.1 Stratigraphy, sampling and stable isotope analyses

In the current study we present new results from a \sim 13.1 m-thick lacustrine interval recovered in the upper part of the \sim 60 m borehole described by [Regattieri et al. \(2015\)](#), which extends to \sim 40 m of the outcrop depth of the previous investigation ([Fig. 1](#)). At this depth (corresponding to \sim 23 m in core, [Fig. 1](#)), the lacustrine succession is interrupted by a hydromorphic paleosol with an upper Hist horizon, which marks the lowermost horizon investigated here. Below this pedogenic horizon (\sim 1 m deep), the sedimentary succession continues, first with a thin layer of gravel and then, continuously to the core bottom, with greyish-greenish lacustrine-palustrine marls ([Fig. 1](#)). However, there are no chronological constraints to allow us to define either the length of the sedimentary hiatus (represented by a paleosol and gravel) or the age of the underlying lacustrine-palustrine sediments, which could be tentatively attributed to a generic MIS 6 ([Fig. 1](#)). Thus, the interval below the peat layer is not discussed further.

The core was sampled at a resolution of \sim 10 cm between 10.2 and 14.8 m and \sim 5 cm between 14.8 and 23.3 m (a total of 13.1 m), which together correspond to the interval between 31.5 and 39.9 m of the outcrop depth ([Fig. 1](#)). Samples for stable isotope analyses were prepared following the procedure described in [Regattieri et al. \(2015, 2016b\)](#). Measurements were made with an Analytical Precision AP2003 continuous-flow isotope-ratio mass spectrometer (IRMS) at the University of Melbourne, Australia, using the same method as described in [Regattieri et al. \(2015\)](#). Briefly, samples were digested in 105% phosphoric acid at 70 °C. Mass spectrometric measurements were made on the evolved CO₂. Results were normalized to the Vienna Pee Dee Belemnite scale using an internal working standard (NEW1, a Carrara Marble), calibrated against the international standards NBS18 and NBS19. Average analytical precision on internal standards was \pm 0.10‰ and \pm 0.05‰ for $\delta^{18}\text{O}$ and $\delta^{13}\text{C}$ respectively.

3.2.3.2 Elemental and mineralogical analyses

X-ray fluorescence spectrometry (XRF) and X-ray powder diffraction (XRPD) analyses were performed at the Earth Sciences Department of the University of Pisa (Italy) using leftover powders of the stable isotope analyses. XRF analyses were conducted at a resolution of ~ 25 cm. A NITON XL3t GOLDD + hand-held XRF unit (HHXRF) was used. Characteristics and performance of the NITON XL3t is described in [Gemelli et al. \(2015\)](#) and the analytical procedure for sediment samples in [Regattieri et al. \(2016b\)](#).

X-ray powder diffraction (XRPD) analyses were performed on 23 unevenly spaced samples ([Fig. 2](#)), using a Bruker D2 Phaser diffractometer equipped with a Lynxeye fast detector. Diffraction patterns were analysed with the Bruker DIFFRAC-EVA software, both for phase identification and for semi-quantitative estimation of mineral abundances through the comparison of measured peak areas.

Field Emission Scanning Electron Microscopy (FESEM) imaging of three samples ([Fig. 2](#)) was performed with a Bruker QUANTA FEG 450 housed at the Department of Civil and Industrial Engineering of the University of Pisa (Italy).

3.3.3.3 Biogenic Silica and sedimentological analyses

Biogenic silica (bSi) concentrations were measured using Fourier transform infrared spectroscopy (FTIRS) at the Institute of Geological Sciences, University of Bern, Switzerland using the method described in [Vogel et al. \(2008\)](#) and [Rosén et al. \(2010\)](#). Calibration followed [Meyer-Jacob et al. \(2014\)](#). Approximately 0.011 ± 0.0001 g of powdered sample was mixed with 0.500 ± 0.0005 g of oven-dried spectroscopic grade potassium bromide (KBr, Uvasol®, Merck Corp.) and subsequently homogenized using a mortar and pestle. A Bruker Vertex 70 equipped with a liquid-nitrogen-cooled MCT (mercury-cadmium-telluride) detector, a KBr beam splitter, and a HTS-Xt accessory unit (multisampler) was used. Each sample was scanned 64 times at a wavenumber resolution of 4 cm^{-1} (reciprocal centimetres) for the wavenumber range 520 to 3750 cm^{-1} in diffuse reflectance mode. FTIR spectra were normalized using a linear baseline correction by setting two defined points of the recorded spectrum to zero (3750 and 2210 – 2200 cm^{-1} , respectively) prior to extracting information on bSi concentrations. Estimates of accuracy and precision of the method are provided in [Meyer-Jacob et al. \(2014\)](#) and [Vogel et al. \(2016\)](#).

3.4.3.4 $^{40}\text{Ar}/^{39}\text{Ar}$ dating and age modelling

A bulk sample of POP4 tephra was collected at the base of the trench described by [Regattieri et al. \(2015\)](#) and dated by $^{40}\text{Ar}/^{39}\text{Ar}$ methods to obtain an independent age. Twenty pristine sanidine crystals in the size range 300 – $400 \mu\text{m}$ were handpicked under a binocular microscope. To remove the attached groundmass, they were slightly leached for 5 min in 7% HF acid. A total of 20 crystals were loaded in a single pit hosted in an aluminium disk and irradiated for 30 min (Irr 95) in the B1 tube of the OSIRIS reactor (French Atomic Energy Commission, Saclay, France). After irradiation, 13 single crystal were transferred into individual pit hosted in a copper sample holder and then loaded into a differential vacuum Cleartran® window. After slight leaching using a 25% W CO₂ laser (Synrad®) at 3.0% of the full laser power, the 13 individual sanidine crystals were fused at about 12% of the full laser power. The Ar isotopes were analysed using a VG5400 mass spectrometer equipped with a single ion counter (Balzers® SEV 217 SEN), following the procedures outlined in [Nomade et al. \(2010\)](#). Neutron fluence (J) was monitored by co-irradiation of Alder Creek sanidine standard (ACS-2, [Nomade et al., 2005](#)). The J value was determined from analyses of three ACS-2 single grains and calculated using an age of 1.193 Ma ([Nomade et al., 2005](#)), and the total decay constant of Steiger and Jäger (1977) (i.e., $J = 3.515 \cdot 10^{-4} \pm 1.410 \cdot 10^{-6}$). Mass discrimination was assessed by analysis of Air pipette throughout the analytical period, and was calculated relative to a $^{40}\text{Ar}/^{36}\text{Ar}$ ratio of 298.56 (Lee et al., 2006). Several proposed calibrations of the $^{40}\text{Ar}/^{39}\text{Ar}$ chronometer are currently in use, yielding ages that vary by ~ 1% ([Kuiper et al., 2008](#); Renne et al., 2011; Jicha et al., 2016). This implies a difference in the calibrated age for our samples within the reported total uncertainty. However, because previous $^{40}\text{Ar}/^{39}\text{Ar}$ ages have been published using these values ([Regattieri et al., 2015, 2016b](#)), we chose to keep them for the current investigation. Procedural blanks were measured every two or three unknowns, depending on the sample beam size previously measured. For a typical 10-min static blank, the backgrounds were generally about 2.0 – $2.2 \cdot 10^{-17}$ and 5.0 – $6.0 \cdot 10^{-19}$ mole/mol for ^{40}Ar and ^{36}Ar , respectively. Full analytical procedures are described in [Nomade et al. \(2010\)](#).

The age model ([Fig. 3](#)) and corresponding 95%-confidence limits were calculated with Clam 2.0 software ([Blaauw, 2010](#)), written in the open-source statistical environment R (R Development Core Team, 2010). Tephra ages in years before present ([Table 1](#)) were used and a smoothing-spline function was applied for interpolation between each age control point. Smoothing was set to 0.7 in CLAM (a smoothing of 0 is used for variable sedimentation rate, which produces a very flexible age model, whereas a smoothing of 1 equals linear interpolation between ages, corresponding to constant sedimentation rate). The age control points (tephra layers) in the upper part of the sequence do not indicate major changes in sedimentation rate. A homogeneous lithology throughout the succession implies a rather constant sedimentation rate, which was used for age-depth [modeling/modelling](#) as a basic assumption, where age control points were lacking (cf. [Fig. 3](#)).

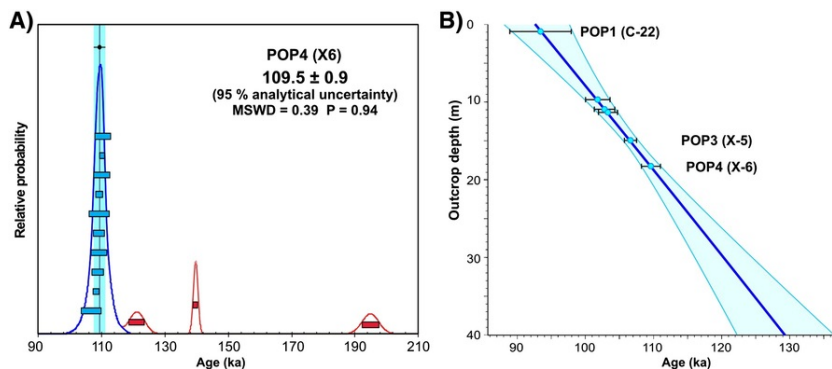


Fig. 3 A) Age probability density spectra for the POP4 tephra. Blue and red bars are the individual ages (1σ error) included and not included in the weighted mean age calculation, respectively; B) age-depth model and tephra control points for the POP succession. Blue line indicates the modelled median age and light-blue lines indicate 95% confidence limits. All tephra ages are modelled ages (see Table 1). (For interpretation of the references to colour in this figure legend, the reader is referred to the web version of this article.)

alt-text: Fig. 3

4.4 Results and discussion

4.1.4.1 $^{40}\text{Ar}/^{39}\text{Ar}$ dating and chronology

Full analytical details for the 13 individual crystals analyses are given in Supplementary Table S1. Age-probability density spectra with individual single crystal age are presented Fig. 3. Among the 13 crystals analysed, ten yielded a similar age. These juvenile crystals allowed calculation of a weighted mean age of 109.5 ± 0.9 ka (2σ analytical uncertainty, $P = 0.94$).

The age model provided in Fig. 3 is based on the tephra layers discussed previously by Giaccio et al. (2012) and Regattieri et al. (2015). Ages for five of these six tephra layers are the same as those used for the age model of Regattieri et al. (2015) (Table 1). For tephra POP4, the new $^{40}\text{Ar}/^{39}\text{Ar}$ age of 109.5 ± 0.9 ka is employed. Due to the difference between the new direct (109.5 ± 0.9 ka) and indirect (108.9 ± 1.8 ka; Iorio et al., 2014) $^{40}\text{Ar}/^{39}\text{Ar}$ ages of the POP4/X-6 tephra, and the different age-modelling approaches, the updated age model for the published section is slightly different from the previous model. However, both models are statistically indistinguishable, as all the differences are well within the associated uncertainties. The new age model spans from 92.5 ± 4.8 ka to 129.2 ± 6.9 ka and the resulting average temporal resolution of the record is ~ 90 years (from 91.7 ka to 121.6 ka) and ~ 50 years (from 121 ka to 130.0 ka) for stable isotope series, ~ 250 years for XRF results, and ~ 1 kyr for bSi. The relatively large uncertainty in the bottom part of the record is due to the lack of control points below the tephra POP4. Consequently, between ca. 110 and ca. 129 ka the age model is statistically extrapolated under the assumption of rather constant sedimentation rate (see Materials and methods). To support our approach, it is worth mentioning that at Sulmona a rather stable sedimentation rate was observed also during the well-dated MIS 19 period; with no major changes between the full interglacial and the glacial inception (max 19% of variations for the ca. 770–758 ka interval, cf. Fig. 1 of Giaccio et al., 2015a, 2015b). Moreover, ongoing stratigraphic and chronological investigations on other intervals of the Sulmona succession also suggest rather constant sedimentation for the MIS 11 and the MIS 13 intervals (our unpublished data).

4.2.4.2 Lithology and mineralogy

As for the previously studied interval (Regattieri et al., 2015), the core is composed of greyish-to-whitish, faintly-to-well-bedded calcareous marl (CaCO_3 content between 80% and 20%, following the classification by Freytet and Verrecchia, 2002). FESEM investigations indicate that the carbonate fraction is mainly composed of euhedral to sub-euhedral calcite crystals of $\sim 3\text{--}5$ μm (Fig. 2). The size and morphology of the crystals are typical of authigenic endogenic calcite, i.e. of carbonates precipitated directly from DIC of the lake water, mostly through algal fixation of CO_2 , influenced by physical conditions, such as hydrology and temperature (e.g. Kelts and Hsü, 1978; Talbot, 1990; Kelts and Talbot, 1990; Leng and Marshall, 2004; Gierlowsky-Kordesch, 2010). FESEM investigations also show an abundance of diatom remains and rare, rounded, coarser clasts of quartz (Fig. 2). Freshwater shells and ostracods (Mazzini et al., in prep.) are also present throughout the core, demonstrating the continuity of lacustrine conditions. Carbonate coatings and/or calcareous charophytes remains were not detected, suggesting that the coring site was not influenced by littoral conditions. Overall, the lithology of the whole POP succession is highly homogeneous, suggesting that no major changes in the deposition environment happened during the covered time interval. Organic matter is virtually absent in the outcropping interval, due to subaerial oxidation, and is < 1 wt% for the core section. X-ray diffraction (XRD) analyses (Fig. 2) reveal that the prominent mineral phase in all samples is calcite, followed by minor quartz. Low-angle low-intensity XRD peaks indicate the presence of very minor amounts of phyllosilicates. In one sample, occurring at 127.5 ka, traces of gypsum were found.

4.3.4.3 The $\delta^{18}\text{O}$ record and its paleohydrological significance

4.3.1.4.3.1 Background

Stable isotope composition of oxygen ($\delta^{18}\text{O}$) of continental carbonates (lacustrine marl and speleothem) depends on isotopic composition of the precipitating solution (drip or lake water) and deposition temperature (e.g. Kim and O'Neil, 1997). According to the main processes supposed to affect the oxygen isotope fractionation, the $\delta^{18}\text{O}$ of carbonates is assessed as a proxy for paleotemperature and paleorainfall amount. The latter is considered to be the dominant process driving $\delta^{18}\text{O}$ in the Mediterranean region (e.g. Bar-Matthews et al., 2000, 2003; Bard et al., 2002; Zanchetta et al., 2007a, 2014, 2016a), together with precipitation/evaporation (P/E) ratio in lacustrine settings (e.g. Roberts et al., 2008; Zanchetta et al., 1999, 2007b, 2012). Carbonate $\delta^{18}\text{O}$ records from the central Mediterranean region also tend to show overall similarities with North Atlantic marine-sediment and Greenland ice-core records, indicating a strong teleconnection between North Atlantic temperature and ocean circulation patterns and Mediterranean hydrology (Drysdale et al., 2004, 2005, 2006, 2007, 2009; Regattieri et al., 2014a, 2014b, 2016a, 2016b; Zanchetta et al., 2012, 2014, 2016a, 2016b). It has also been proposed that the hydrological significance of $\delta^{18}\text{O}$ of Mediterranean continental carbonates can be offset by the effects of changes in the isotopic composition of the sea source (Rohling et al., 2015; Marino et al., 2015). This effect can be particularly important during major climatic shift, such as a deglaciation, when the decrease in planktonic $\delta^{18}\text{O}$ due to ice melting precedes the rise in sea-surface temperature (SST). However, multi-proxy studies from lake sediments and speleothems show variations in recharge-sensitive chemical and lithological properties synchronous with $\delta^{18}\text{O}$ changes, confirming the hydrological significance of $\delta^{18}\text{O}$ (Drysdale et al., 2009; Regattieri et al., 2014b, 2016a, 2016b). Another factor that can affect the $\delta^{18}\text{O}$ of continental carbonates is a change in the relative proportion of Mediterranean (^{18}O -enriched) versus North Atlantic (^{18}O -depleted) precipitation. During cold periods, the strengthening of the north-westerly wind system would cause strong airflows through the passages between the Pyrenees, the Massif Central and the Alps, carrying cold and dry polar or continental air masses to the Gulf of Lyon. This favours cooling and evaporation of surface water masses in the western Mediterranean, leading to enhanced formation of Western Mediterranean Deep Water (WMDW) and stronger thermohaline circulation in the basin (Cacho et al., 2000). This mechanism acts in an opposite direction with respect to North Atlantic, where marine records indicate a reduced MOC during cold periods (e.g. Rasmussen et al., 1996; Curry and Oppo, 1997; Vidal et al., 1997). A higher proportion of vapour masses forming within the Mediterranean would have produced precipitation with higher $\delta^{18}\text{O}$, owing to reduced rainout fractionation and evaporation from a more isotopically enriched water mass compared to the North Atlantic. This fact has been also noted in several studies of present day precipitation (e.g. Celle-Jeanton et al., 2001). On the other hand, during warm periods WMDW formation is depressed while MOC is enhanced, leading to greater evaporation from the more isotopically depleted North Atlantic. This would produce a higher proportion of meteoric precipitation, having lower $\delta^{18}\text{O}$ values, exacerbated due to the higher rainout fractionation.

In previous studies on lacustrine carbonates from the Sulmona Basin, the $\delta^{18}\text{O}$ composition was interpreted as a proxy for precipitation amount in the high-altitude catchment of the karst recharge system (Giaccio et al., 2015a; Regattieri et al., 2015, 2016b), with higher (lower) $\delta^{18}\text{O}$ values related to drier (wetter) conditions. The influence on the final $\delta^{18}\text{O}$ of local precipitation and evaporation directly within the lake are considered to be of little relevance due to the large discharge of the karstic springs feeding the lake. On the other hand, increased evaporation under drier conditions favours the deposition of lake carbonates with higher $\delta^{18}\text{O}$ values, thus acting in the same direction of the amount effect.

Due to the extensive outcrop of carbonate bedrock in the Sulmona watershed (Fig. 1), it may be argued that detrital carbonate from the catchment may constitute an important component of the sediment. This would imply that changes in the clastic input could affect the $\delta^{18}\text{O}$ composition of the bulk sediment independently of the hydrological signal discussed above (e.g. Leng et al., 2010). Following the recommendations of Roberts et al. (2008), to exclude such contamination catchment carbonate rocks need to be sampled and measured isotopically for comparison. In previous work on Sulmona spanning the MIS12-MIS11 interval, the comparison of isotope values from lacustrine marls and gravels from cores and nearby outcrops of marine carbonate bedrock shows that there is no significant mixing between detrital and authigenic endogenic calcite (Regattieri et al., 2016b). In Figure 4, $\delta^{18}\text{O}$ values for the MIS5 interval are reported along with those from the MIS12-11 interval (Regattieri et al., 2016b) and from the MIS19 interglacial (Giaccio et al., 2015a). These data are compared with isotope values of gravels from the Sulmona basin and carbonate alluvial deposits from the nearby Valle Giumentina (Villa et al., 2016), which drains the same Meso-Cenozoic carbonate domain. This extended comparison confirms the previous results: isotope values from the lacustrine carbonates can be readily discriminated from those of the catchment (Fig. 4), thus supporting the hypothesis that the authigenic endogenic calcite $\delta^{18}\text{O}$ signal dominates even when the clastic fraction is abundant, and that the variations observed are not due to mixing between allogenic (clastic) and authigenic endogenic (bio-mediated) carbonate.

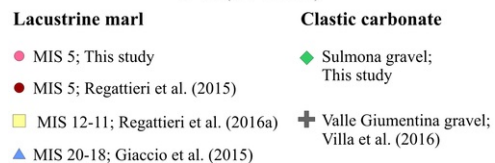
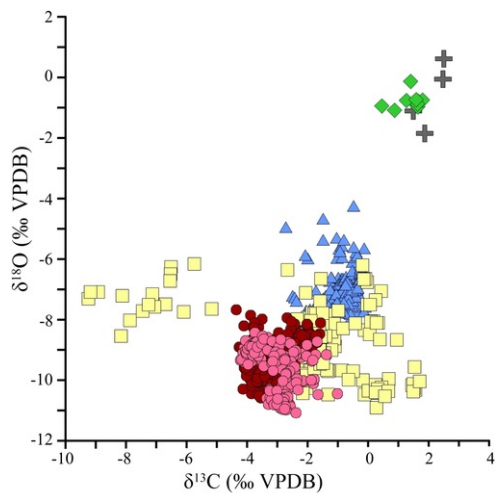


Fig. 4 Comparison of stable isotope values from Sulmona lacustrine sediments related to different stratigraphic units and temporal intervals and carbonate bedrock-clastic material from Sulmona Basin and the nearby Valle Giumentina (15 km East from POP section, [Villa et al., 2016](#)), carved in the same Meso-Cenozoic marine carbonate series.

alt-text: Fig. 4

Previously, the millennial variability of the δ¹⁸O record of the POP section for the ca. 90–115 ka interval ([Regattieri et al., 2015](#)) was shown to be consistent with the patterns of Greenland Interstadials (GI) 25 to 23 (NGRIP members, 2004) and North Atlantic cold events C24-C23 (McManus et al., 2004), indicating a close phase relationship between the early Last Glacial paleoclimate variability of both regions. The POP record for the early Last Glacial also shows a prominent interval of negative δ¹⁸O values corresponding to the GI24 event (108.0–105.1 ka). The higher amplitude of this oscillation, with respect to the Greenland δ¹⁸O record and to speleothem δ¹⁸O records from the Alps, both interpreted in terms of temperature (NALPS, [Boch et al., 2011](#)), was suggested to be related to enhanced seasonality of the climate (dry summer and wet winter) causing an annual bias toward ¹⁸O-depleted winter precipitation and thus more negative calcite δ¹⁸O ([Regattieri et al., 2015](#)).

4.3.2.4.3.2 The 115–129 ka δ¹⁸O record

Stable isotope results plotted versus depth and versus age are presented in [Figs. 2 and 5](#), respectively.

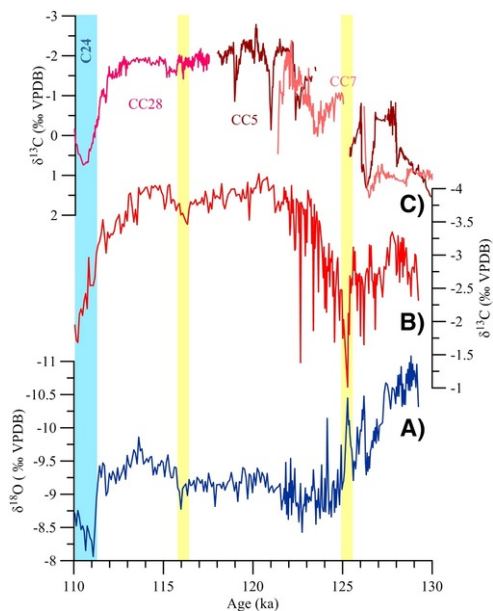


Fig. 5 POP stable isotope results plotted vs. age. A) $\delta^{18}\text{O}$, B) $\delta^{13}\text{C}$ (red). $\delta^{13}\text{C}$ composition of speleothems (CC5, CC7 and CC28) from Corchia Cave (Drysdales et al., 2007, 2009, C). Yellow bars indicate events discussed in the text and blue bar indicates the event C24 (as defined on POP succession by Regattieri et al., 2015). [\(For interpretation of the references to colour in this figure legend, the reader is referred to the web version of this article.\)](#)

alt-text: Fig. 5

In this new presented interval (~ 27 to 40 m of the outcrop depth, Fig. 1; from 117.8 to 129.2 ka, Figs. 2 and 5), $\delta^{18}\text{O}$ ranges from -10.58‰ and -7.68‰ . The $\delta^{18}\text{O}$ record starts with more negative values, which, based on the above-mentioned interpretation, indicate enhanced precipitation and potentially stronger seasonality lasting until 127.3 ka. Between 127.3 ka and 126.3 ka an abrupt rise in isotope values is related to decreasing precipitation and/or decreasing seasonality. It is followed by two short (~ 0.5 kyr) wetter reversals centered at 126.2 ka and 125.3 ka and by a steep trend of increasing values until ca. 125 ka. From ca. 125 to 117.8 ka the record shows higher but more stable $\delta^{18}\text{O}$ values (Fig. 5). Less prominent and shorter events (~ 0.5 kyr) of reduced precipitation are apparent at 122.7 ka, 119.1 ka, and 116.0 ka (Fig. 5). It is worth mentioning that the ages attributed to these events are limited by the uncertainties associated with the age model. However, such uncertainties affect to a lesser extent the age differences and therefore the length and the temporal spacing of these short climatic events.

4.4.4.4 The carbon isotope record

In the newly presented interval, the $\delta^{13}\text{C}$ ranges from -4.35‰ to -1.57‰ , with a mean value of -3.41‰ (Figs. 2 and 5). The record starts with an interval of values around -3‰ and with a high multi-decadal to centennial-scale variability. At ca. 126 ka there is an abrupt, brief positive excursion, followed by a steep decrease until ca. 122 ka, after which values remain relatively stable before the marked dry interval correlated to the C24 ocean cooling event at ca. 110 ka (Regattieri et al., 2015), but with brief low-amplitude increase at ca. 116 ka (Fig. 5).

Factors influencing the isotopic composition of DIC in karstic lakes are numerous (Hollander and McKenzie, 1991; Leng and Marshall, 2004; Mayer and Schwark, 1999; Zanchetta et al., 2012). In general, ^{13}C -depleted intervals reflect an increased input of CO_2 derived from oxidation of organic matter within the lake and/or leaching of soil-derived CO_2 from the catchment (e.g. Mook and Tan, 1991). On the other hand, higher $\delta^{13}\text{C}$ values suggest increasing equilibration with atmospheric CO_2 and/or contribution from bicarbonate originating from the dissolution of limestone, and/or increased ^{12}C consumption by biological activity within the lake (e.g. Zanchetta et al., 2012). Influencing most of these above-mentioned factors are variations in hydrological conditions, such as changes between open and closed system. These are key drivers for changes in $\delta^{13}\text{C}$ composition (e.g. Roberts et al., 2008) and need to be addressed thoroughly before to make any attempt to interpret the $\delta^{13}\text{C}$ record in terms of past climate variability. However, Sulmona is a paleo-lake, so past hydrology is difficult to constrain and cannot be fully inferred from present-day conditions. Thus, we stress that the interpretation of the $\delta^{13}\text{C}$ record proposed here is based on current theory in the context of local physical setting. In the majority of the interval previously discussed by Regattieri et al. (2015), from ca. 98 to 110 ka, and in the new record back to ca. 122 ka, the $\delta^{13}\text{C}$ closely tracks $\delta^{18}\text{O}$ (Fig. 5). It may suggest that the evolution of the DIC of the lake follows regional precipitation changes and the local E/P ratio. Covariations between $\delta^{18}\text{O}$ and $\delta^{13}\text{C}$ in fact can be explained by: *i*) changes in soil development/productivity, promoted by rainfall-induced vegetation cover changes, and thus by changes in the amount of soil CO_2 entering in the karst system (e.g.

Lézine et al., 2010); or *ii*) to increased water residence time in the lake, which promotes evaporation (causing ^{18}O -enrichment) and equilibration of the DIC with atmospheric CO_2 (causing higher ^{13}C). The $\delta^{13}\text{C}$ record between ca. 129 ka and ca. 122 ka instead decouples from the $\delta^{18}\text{O}$. In detail, it is possible to define two intervals within this period: from 129.2 ka to ca. 125 ka mean $\delta^{13}\text{C}$ values are higher (Fig. 5) with respect to the subsequent portion of the LIG. However, there is a decreasing trend which mimics that of the $\delta^{18}\text{O}$, with a covariant increase at \sim ca. 127.3 ka. Conversely, at the centennial scale, the two curves are anti-correlated (Fig. 4). For the period between ca. 125 ka and ca. 122 ka, by contrast, the $\delta^{13}\text{C}$ values decrease rapidly and the anti-correlation with $\delta^{18}\text{O}$ is more persistent. Lower $\delta^{13}\text{C}$ values for the interval ca. 129–125 ka can potentially be explained by a muted soil development, and thus by a low amount of CO_2 from OM respiration/oxidation, in the high altitude recharge area of the karst system. A delayed development of soils in high altitude sites at the beginning of interglacial periods has already been inferred from speleothems $\delta^{13}\text{C}$ records from Corchia Cave in central Italy, both for the LIG (Drysdales et al., 2005, 2009, Fig. 5) and for the Holocene (Zanchetta et al., 2007a). The lag observed in the POP record is comparable to that of Corchia (2–3 kyr), as is the altitude of the recharge areas of the two sites (1200–1500 for Sulmona and \sim 1200 m a.s.l. for Corchia). Also at Sulmona, it is likely that glacier cover and erosion and/or sparse alpine vegetation cover may have hampered soil development during the early LIG, leading to a persistent contribution of ^{13}C -enriched atmospheric and bedrock carbon to the dissolved load of the karst aquifers. The short-term anti-correlation is more difficult to address. One likely explanation is that it is related to short-term increases in the proportion of waters originating from the karst system. Indeed, increased precipitation in the mountains (^{18}O -depleted) could trigger periods of karst system overflow, with injections of waters loaded with enriched $\delta^{13}\text{C}$ and originated from intermittently active sectors of the recharge system, that supply older water having longer interactions with the bedrock.

4.5.4.5 Elemental and mineralogical composition of the sediment

4.5.1.4.5.1 XRF

The depth and temporal series of the analysed elements (Ti, Rb, Zr, Al, Si, Ca, Sr) are shown in Figs. 2 and 6, respectively. Correlation coefficients are reported in Table 2 while scatterplots are reported in supplementary Fig. S1.

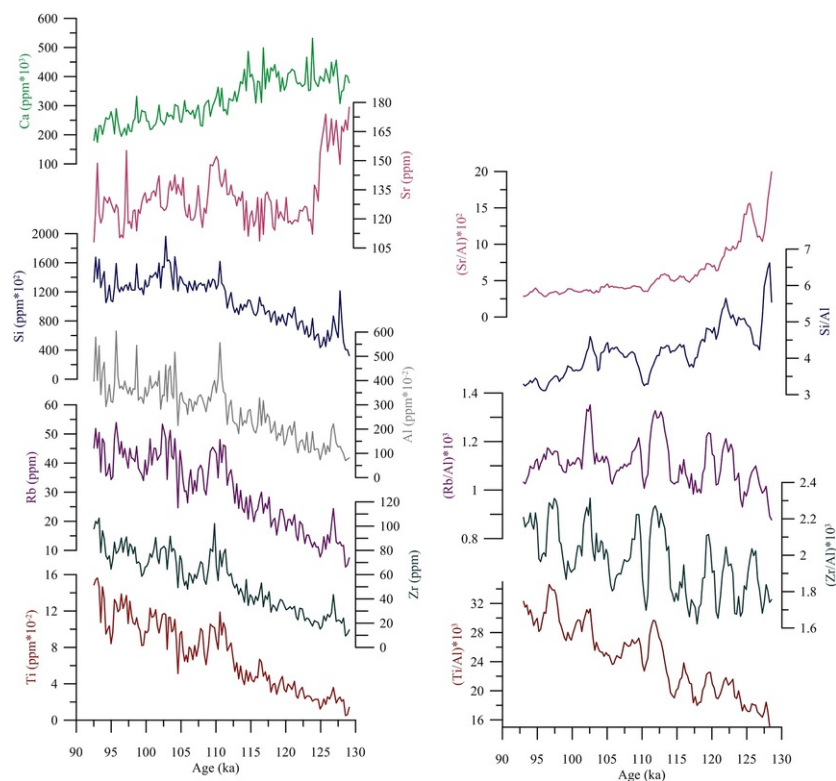


Fig. 6 Left panel: XRF results plotted vs. age (from bottom: Ti, Zr, Rb, Al, Si, Sr, Ca); right panel: Five-point smoothed time series of normalized XRF data (from bottom: Ti/Al, Zr/Al, Rb/Al, Si/Al, Sr/Al).

Table 2 Pearson correlation coefficients (r) between elements concentration (XRF data, n_i=141)

alt-text: Table 2

	Ca					
Sr	+ 0.17	Sr				
Ti	- 0.85	- 0.29	Ti			
Zr	- 0.85	- 0.25	+ 0.98	Zr		
Rb	- 0.79	- 0.27	+ 0.96	+ 0.97	Rb	
Si	- 0.67	- 0.35	+ 0.86	+ 0.86	+ 0.90	Si
Al	- 0.65	- 0.29	+ 0.91	+ 0.89	+ 0.93	+ 0.92

Ti, Rb, Zr, Al and Si variations are commonly linked to siliciclastic/detrital input to the lake and are associated also with grain-size variations (Koinig et al., 2003; Kylander et al., 2011; Vogel et al., 2010). They are usually considered as proxies for the intensity of wind (Zr) and/or of erosion in the lake catchment (Ti, Rb, Al, Si), increases of which are usually related to a reduction in vegetation cover, an increase in soil erosion, and/or increased wind intensity (e.g. Vogel et al., 2010; Kylander et al., 2011). Increases in all of these elements can also result from a closer proximity of the shoreline to the coring site, i.e., a lower lake level, which also indicates drier climatic conditions. However, an increase in these elements could be also related to increased runoff under wetter conditions (e.g. Francke et al., 2016).

At Sulmona, the lake catchment is mostly composed of carbonate rocks containing only a limited amount of siliciclastic components, which are enriched in elements such as Ti, Rb, Zr, Al and Si. Thus, the most likely source of these elements is volcanoclastic deposits, which are abundant in the whole basin (e.g. Giaccio et al., 2009, 2012, 2013a), as well as small outcrops of Miocene-lower Pleistocene siliciclastic flysch in the NW sector of the basin (Cavinato and Miccadei, 2000), and/or exotic aeolian dust. Si can also be influenced by the presence of biogenic silica (bSi), which is the main component of diatom frustules, and ranges from 13% wt% to 2% wt% in the studied interval (Section 4.6). Ca occurs mostly as endogenic/ authigenic calcite, as revealed by XRD and FESEM analyses (Fig. 2 and Section 4.2.1). Thus, Ca content can be seen as an indirect proxy for lake primary productivity. Sr can be either transported along with the detrital fraction, as it is abundant in volcanoclastic deposits, or may substitute Ca in carbonates. The low negative correlation of Sr with Ti, Zr, Rb and Si (Table 2, r values ranging from - 0.25 to - 0.35) and the weak positive correlation between Sr and Ca (r_i=0.17) indicate that the Sr content is at least partly related to either detrital input or co-precipitated as a divalent ion replacement for Ca in endogenic/ authigenic and biogenic calcite.

Ti, Rb, Si, and Zr all show strong positive correlations (r values ranging from 0.86 and 0.97, Table 2) and a similar trend of increasing values throughout the record (Fig. 6). However, the agreement between these elements must be evaluated by considering the dilution effect related to the decreasing trend of CaCO₃, which ranges from 85% to 40% from the base to the top of the sequence. Variations in Ca content, which is mostly related to calcite precipitation, can affect the relative concentrations measured for other elements and, as a matter of fact, Ca is strongly negatively correlated with all the above-mentioned elements (r values ranging from - 0.67 and to - 0.85, Table 2). However, it is important to note that these negative correlations are not an analytical artefact: they are consistent with climate-driven processes. Colder and drier conditions trigger an increase in detrital input due to enhancement of soil erosion promoted by reduced vegetation cover, leading to dilution of the CaCO₃ content. In addition, the precipitation of authigenic/ endogenic carbonates, which is at least partly controlled by water temperature and primary productivity, is reduced under conditions of climate deterioration. For example, cooler lake waters hold more CO₂ and HCO₃ in solution than warmer lake waters, and generally have a lower ionic strength due to decreased dissolution rates in the catchment. This culminates in lower levels of carbonate ion activity and supersaturation during cold stages, leading to lower rates of calcite precipitation. Conversely, wetter and warmer periods promote denser vegetation cover and enhanced soil development, which reduces detrital flux from the catchment. These conditions and also increased lake primary productivity, decreased CO₂ solubility in the water, all of which promote higher rates of authigenic calcite precipitation.

An approach which is traditionally used to overcome the dilution effect is the normalization of element concentrations by a conservative, lithogenic element (e.g. Kylander et al., 2011, 2013 Löwemark et al., 2011; Vogel et al., 2010). In many cases, normalization allows one to identify misleading trends in element concentrations. The element to be used for normalization should not itself be a proxy nor be affected by biological or redox processes (Löwemark et al., 2011). Ti is widely used for normalization as it is a common accessory component in various mineral phases and is conservative in terms of its reactivity. However, Ti is enriched in heavy minerals and in aeolian dust, and in particular settings it can therefore be used as a proxy for high-current regimes (Schnetger et al., 2000) or enhanced wind activity (Wehausen and Brumsack, 1999; Yancheva et al., 2007). Another element suitable for normalization is Al (Löwemark et al., 2011), which is a major component of siliciclastic mineral phases and, similar to Ti, is not significantly affected by redox and biologically mediated reactions (Brumsack, 2006). Once this approach is applied to our XRF series, the correlation coefficients between Zr/Al, Ti/Al and Rb/Al, which are exclusively of detrital origin, remain high (Table 3, Fig. S2), and the increasing long-term trend in element ratios compares well with element

concentrations from ca. 129 ka to 92 ka (Fig. 6). Thus, normalization using Al confirms the exclusively detrital origin for Zr, Ti and Rb, and that the observed long-term trends are not an artefact caused by CaCO₃ dilution. Specifically, all three ratios show a twofold structure, with an older (up to ca. 115 ka) part displaying a lower clastic input and a younger part (90–115 ka) with a higher sediment delivery. They also show clear maxima at ca. 111 ka and 103 ka, corresponding to periods of higher δ¹⁸O values, which we interpret as indication of drier conditions.

On the other hand, normalization of Si vs. Al causes correlation coefficients amongst clastic elements to decrease, and highlights a decreasing Si/Al trend throughout the observed period. Because normalization vs. a lithogenic element may remove the influence of mineral input to the lake (Kylander et al., 2013), variations in Si/Al can be seen as reflecting the contribution of the deposition of biogenic silica. It is also worth noting that correlations between Sr/Al and Si/Al and between Sr/Al and Ca/Al increase (to 0.61 and 0.95 respectively, Table 3), and that Sr/Al also shows a decreasing trend that mimics that of Ca and Si, supporting the notion that part of the Sr is related to co-precipitation of Sr within the authigenic calcite as SrCO₃ (Table 3).

Table 3 Pearson correlation coefficients (r) between elements/Al ratios (n = 141).

alt-text: Table 3

	Zr/Al					
Rb/Al	+ 0.84	Rb/Al				
Ti/Al	+ 0.77	0.66	Ti/Al			
K/Al	+ 0.58	0.67	+ 0.17	K/Al		
Si/Al	- 0.02	0.04	+ 0.36	+ 0.49	Si/Al	
Sr/Al	- 0.03	0.06	+ 0.51	+ 0.48	+ 0.61	Sr/Al
Ca/Al	+ 0.19	- 0.52	+ 0.66	- 0.47	+ 0.65	+ 0.95

Now that normalization of clastic-elements vs. Al confirms the observed trends and correlations noted above, and considering the abovementioned potential causal negative relationship between calcite deposition and detrital clastic input, we can now discuss the original elemental time series in terms of paleoenvironmental changes. As a further step, in order to identify only significant and potentially climate-driven changes and to avoid overestimating variations in individual elemental concentrations using a merely visual approach, we can statistically combine Ti, Zr and Rb to produce a “clastic index” (CI hereafter) that can be compared with the stable isotope profile, assuming that all these elements respond in the same way to environmental/climatic forcings (i.e. increasing or decreasing catchment erosion). To do this, the time series of Ti, Zr and Rb were normalized to produce individual time series of anomalies (i.e., deviations from a zero mean expressed in standard deviation units, or standard scores). The standard scores of the three series were averaged to produce a CI time series where low average standard scores correspond to intervals with lower clastic input to the lake, and vice versa. The comparison of the CI with the δ¹⁸O time series reveals a high degree of consistency (Fig. 7), for both the general patterns and short term events. Periods of reduced precipitation inferred from higher δ¹⁸O values are in fact marked by increases in the CI, indicating increased catchment erosion. In particular, the drier events that are correlated with C23 and C24 North Atlantic cold events appear prominent in the CI series, whilst while the events at 127.3 ka and 116.0 ka are expressed by a concomitant rise in the detrital clastic input (Fig. 7). Conversely, lower δ¹⁸O values indicating wetter conditions correspond to reductions in the CI due to increase in soil-vegetation cover, and reduced flux of detrital clastics to the lake. It is worth recalling that both arid and wetter conditions may increase sediment delivery, and that temperature may affects vegetation cover and soil erodibility. However, the good correlation between periods with higher δ¹⁸O and elevated CI values supports the proposed link between drier periods and enhanced catchment erosion.

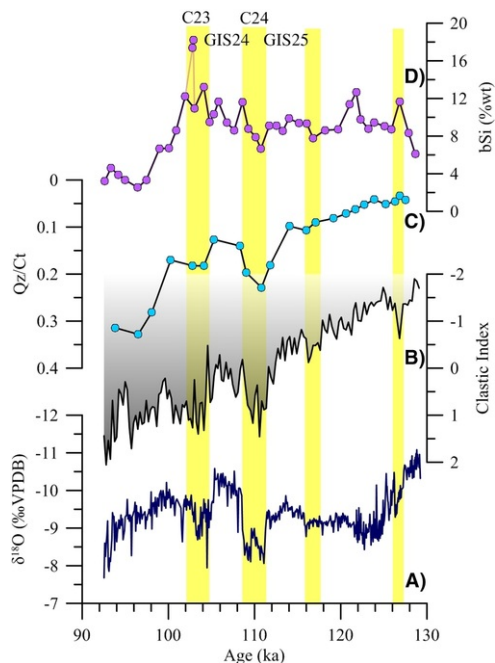


Fig. 7 Comparison of $\delta^{18}\text{O}$ (A); clastic index (CI, see text for explanation; B); quartz/calcite ratio (Qz/Ct, C) and biogenic silica (bSi, D) time series. Yellow bars indicate dry events discussed in the text, GS are Greenland interstadial, as defined in the POP section by Regattieri et al. (2015). (For interpretation of the references to colour in this figure legend, the reader is referred to the web version of this article.)

alt-text: Fig. 7

4.5.2.4.5.2 XRD

Due to the highly monotonous mineralogical composition of the sediments (see Section 4.2), a simple semi-quantitative approach can be applied to XRD data to test if mineralogical variations are also indicative of the same environmental changes revealed by others proxies. As previously discussed, most of the calcite is endogenic/autigenic, while quartz is related to detrital input to the lake. As silicate rocks are present only marginally in the lake catchment, quartz could also have an eolian origin, as suggested for quartz-rich loess deposits along the Apennine (Giraudi et al., 2013) and from lakes in volcanic settings from central Italy (Vico and Lagaccione Lakes; Narcisi, 2000). Plotting the ratio between peak areas of quartz and calcite (Qz/Ct) against both the CI and $\delta^{18}\text{O}$ time series (Fig. 7) the general features of the CI appear well replicated in the Qz/Ct curve, with an increasing trend throughout the interglacial and major peaks corresponding to C24 and C23 events. This similarity seems to confirm the interpretation of the XRF data, showing phases of high/low primary productivity (high/low calcite content) related to reduction/increase in the clastic input to the lake, which also supports a link between sediment mineralogy and climatic conditions. The good correspondence moreover indicates that this simple ratio can be used as a good proxy for the detrital clastic input, with the advantage to be not influenced by potential dilution effects.

4.6.4.6 Biogenic silica

Due to its resistance against post burial degradation/dissolution, bulk biogenic silica (bSi) is commonly used as a proxy to reconstruct past changes in aquatic/algal productivity (Francke et al., 2016; Prokopenko et al., 2006; Vogel et al., 2010) or changes in the delivery of dissolved silica to the lake due to variations in the rate of chemical weathering in the drainage basin (Johnson et al., 2011). In the studied interval, bSi ranges from 2.5 wt% to 18.2 wt% (mean 8.94, SD 3.29), (Figs. 2 and 7). It is worth noting that the two most extreme values occur in closer proximity to tephra POP2a and POP2b (Fig. 2). Tephra influx increases the silica content in the water (Barker et al., 2000) and it has been noted that such fluxes could alter lake water chemistry and benthic habitat. It could cause a shift in diatom assemblages and populations (e.g. Cvetkoska et al., 2015), and/or an increase in diatom productivity (D'Addabbo et al., 2015), and/or an increase in individual diatom frustule size (Jovanovska et al., 2016). Volcanic material is likely the primary source for Si in Sulmona. Thus, tephra deposition or mobilization from the catchment can be an important trigger for diatom blooms and increases in frustule size, largely independent of climate. With this in mind, the two samples with exceptionally high bSi concentrations centered at 102.8 ka and 102.9 ka - close to tephra deposits - can be excluded from the following discussion of climate and environmental change (Fig. 7).

Although the low resolution of the bSi curve (one sample every ~ 1 kyr) prevents a close comparison with the $\delta^{18}\text{O}$ time series, it is interesting to note that there is a decrease in bSi values corresponding to higher isotope values during the cold/dry event C24. Moreover, bSi decreases during the Early Last Glacial from ca. 102 ka onwards, thus mimicking the $\delta^{18}\text{O}$ trend toward higher values. The pattern during the Eemian instead is not very clear, and there is a lack of a well-expressed peak in productivity related to full interglacial conditions. A potential explanation is related to dilution of bSi by increased calcite deposition during the LIG. This seems supported by the Si/Al curve (Fig. 6). Because normalization removes the influence of clastic Si, the highest Si/Al ratio observed during the first part of the LIG, which has no counterpart in the other clastic detrital elements (Ti, Rb, Zr), can be attributed to a higher contribution of bSi to the total Si budget related to a peak in primary productivity under full interglacial conditions. However, higher resolution bSi analyses would be needed to test this hypothesis.

4.7.4.7 Significance of the POP record in the framework of Mediterranean climate variability during the LIG

In order to better frame the POP record in the context of regional climate variability, we can now compare it with existing regional paleoclimate archives, in an attempt to draw a coherent picture of observed variability and to unravel the potential mechanisms driving hydrological and environmental changes, for both long-term trends and short-term events.

Of particular interest is the comparison of the Sulmona $\delta^{18}\text{O}$ profile with speleothem records from Corchia Cave and Tana che Urla Cave (Fig. 8, Drysdale et al., 2007, 2009; Regattieri et al., 2012, 2014a, 2016a). These two records are both located in the western Apennines, ~ 400 km north of Sulmona (Fig. 1). All three oxygen isotope records show a highly coherent pattern of $\delta^{18}\text{O}$ variations with respect to timing and amplitude of the observed changes during the investigated period (Fig. 8). The fact that the precipitation signal is replicated in the three records allows us to discuss changes in $\delta^{18}\text{O}$ in terms of regional expression of the variations of the precipitation amount over the central Mediterranean area. Moreover, the comparison supports the chronology proposed for the POP record, despite the relatively high uncertainty for the lower part of the interval. By considering this good chronological and paleohydrological consistency, the onset of lake conditions in the Sulmona Basin at ca. 129 ka could be conceivably seen as the environmental response to the increase in precipitation which cause the abrupt decreasing of central Italy speleothem $\delta^{18}\text{O}$ at the Eemian onset (129.0 ± 1 ka, Drysdale et al., 2005 and 129.6 ± 1 ka, Regattieri et al., 2016a). Conversely, the peat layer at the bottom of the POP lacustrine succession may be likely related to the initial stages of lake formation during the deglaciation that preceded the Eemian and follows the marked dry event at ca 130.5 ± 129.5 ka documented in Tana che Urla Cave (Regattieri et al., 2014a) and recently reinterpreted as hydrological expression of the North Atlantic Heinrich event 11 (Regattieri et al., 2016a).

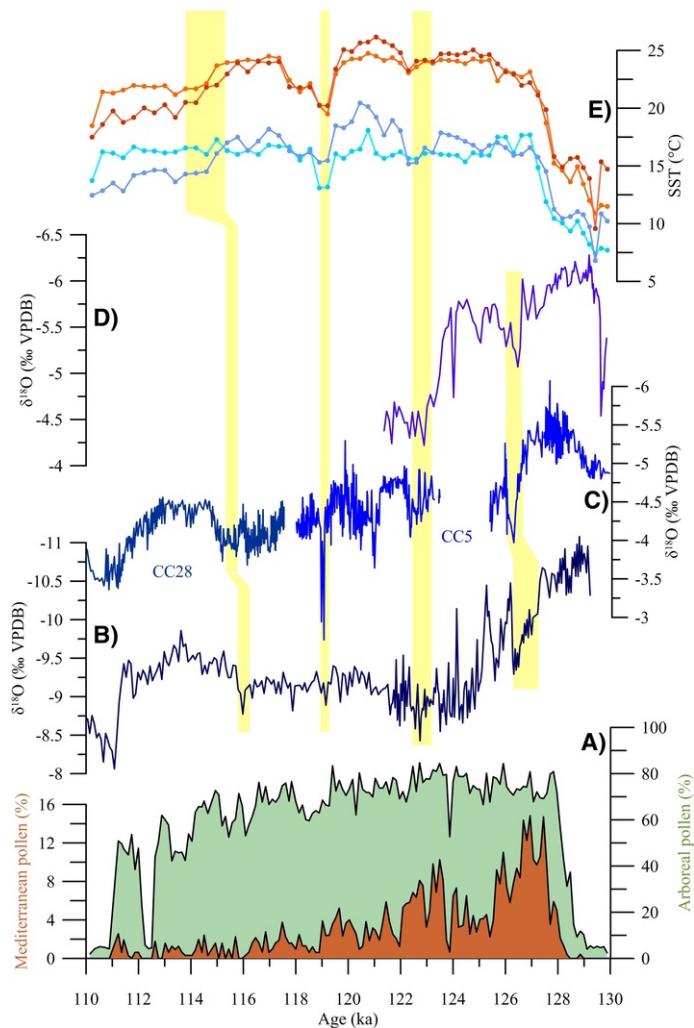


Fig. 8 Comparison of POP and regional paleoclimate records. a) Tenaghi Philippon pollen record (Milner et al., 2013); b) POP $\delta^{18}\text{O}$ record; c) Corchia Cave $\delta^{18}\text{O}$ record (stalagmite CC28, Drysdale et al., 2007, stalagmite CC5, Drysdale et al., 2009); d) $\delta^{18}\text{O}$ record from Tana che Urla Cave (Regattieri et al., 2014a); e) faunal SST record from core ODP-975 (orange, summer temperature; blue, winter temperature; lighter lines are from Modern Analogue technique and darker from Transfer Function technique, Kandiano et al., 2014). Yellow shadings indicate events of reduced precipitation and environmental deterioration. All the compared records are plotted on their published age model. [\(For interpretation of the references to colour in this figure legend, the reader is referred to the web version of this article.\)](#)

alt-text: Fig. 8

In all the three records, the initial part of the LIG (from ca. 129 to ca. 127 ka on the POP chronology) shows a short interval of minimum $\delta^{18}\text{O}$ values (Fig. 8). This interval suggests high precipitation and/or enhanced seasonality, as discussed above. For the early part of the LIG, an enhanced Mediterranean character of the precipitation (i.e., summer drought and precipitation concentrated in autumn and winter) has been highlighted by several paleoclimate records (e.g. Tzedakis et al., 2003; Brauer et al., 2007; Toucanne et al., 2015; Milner et al., 2012) and has been related to the northward migration of the Intertropical Convergence Zone (ITCZ) during precession minima at the time of Sapropel S5 deposition in the eastern Mediterranean (Milner et al., 2012; Toucanne et al., 2015). Notably, the pollen records from Tenaghi Philippon (Greece, Milner et al., 2012, 2013, Fig. 8) show that the early part of the Eemian corresponds to the highest percentage of Mediterranean taxa. The same applies for the pollen record from the Iberian margin marine core MD95-2042 (Sánchez-Goni et al., 1999, 2007). It should be noted that some others

pollen records from the same period, like that from Monticchio and from Ohrid lakes (Brauer et al., 2007; Sadori et al., 2016), do not clearly show a similar increase in Mediterranean vegetation during the early Eemian. However, these records show generally low percentages (i.e. below 15%) of Mediterranean taxa and only minor variations between glacial and interglacial periods; thus likely both sites are not fully suited to discuss variations in this kind of essences in terms of increasing/decreasing seasonality. The link between minimum $\delta^{18}\text{O}$ values and higher seasonality is also supported by the fact that in the POP record neither the CI nor the Qz/Ct ratio show a steep increase at 127.3 ka. It suggests that no abrupt and major changes in catchment erosion, related to major changes in precipitation amount, happened at that time. Rather, an increase in the contribution of isotopically light winter precipitation and/or a substantial reduction in isotopically enriched summer rains would have been able to cause the shift of the annual weighted mean isotopic values of precipitation towards more negative values (Longinelli et al., 2006), affecting $\delta^{18}\text{O}$ calcite values. This seems to be supported also by the fact that the peak corresponding to GI24 in the CI series, although being well expressed, is no more prominent than the previous interstadial (GI25) (Fig. 7). Conversely, in the $\delta^{18}\text{O}$ series GI24 is very pronounced, as almost as the first part of the LIG (Fig. 7), and its prominence was suggested to be due to higher seasonality (Regattieri et al., 2015).

After this short-term optimum, all three $\delta^{18}\text{O}$ records show an abrupt event of reduced precipitation lasting ~ 1 kyr (Fig. 8), which is accompanied in the POP record by a concomitant increase in the CI (Fig. 7), suggesting reduction in vegetation cover and increased catchment erosion. It is interesting to note that also pollen records from southern Italy (Monticchio Lake, Brauer et al., 2007), from Greece (Ioannina, Tzedakis et al., 2003 and Tenaghi Philippon, Milner et al., 2013, 2016) and from the Iberian margin (core MD95-2042, Sánchez-Goñi et al., 1999, 2007, 2005) report a nearly coincident event of reduced arboreal pollen around ca. 127 ka. Thus, together these records seem to support the notion of temporarily regional climate deterioration straight after the beginning of the LIG, although uncertainties related to each age models prevent a secure correlation.

After ca. 126 ka, the POP record shows a trend toward drier conditions and enhanced centennial-scale environmental instability until ca. 125 ka, which is well replicated in regional speleothem and pollen records (Fig. 8). Additional minor centennial-scale dry events in the POP record are centered at ca. 112.7 ka, ca. 116.0 ka and ca. 119.1 ka (Fig. 8). These events are, within chronological uncertainties, also recorded in the Corchia and Tana che Urla speleothems.

Moving to the marine realm, a high-resolution study of faunal and geochemical proxies from the western Mediterranean site ODP-975 recognized several short-term climatic events within MIS5e, which have been assigned to disruptions of the AMOC and associated changes in atmospheric circulation (Kandiano et al., 2014). Particularly, SST reconstructions from foraminifera (developed by Modern Analogue and Transfer Function techniques) show three notable cooling events centered around 122.3 ka, 119.0 ka and 114.2 ka (Fig. 8). These events are consistent with intra-interglacial variability recognized in the western Mediterranean basin (Sprovieri et al., 2006) and mimic intra-interglacial instability emerging from North Atlantic records (McManus et al., 1994; Oppo et al., 2001, 2006; Bauch et al., 2012; Irali et al., 2012). These decreases in SST have recently been proposed to be related to episodic cold water-mass expansions in the North Atlantic and associated southward migration of the Arctic Front (Mokeddem et al., 2014) and/or to changes in North Atlantic Deep Water (NADW) formation due to buoyancy changes related to melting of persisting ice sheets (Galaasen et al., 2014). It has to be noted that the western Mediterranean faunal SST record is lacking clear evidence for the event at ca. 127 ka (Kandiano et al., 2014). However, this event falls within the deposition of an Organic Rich Layer (ORL) and corresponds to peak abundances of the cold dwelling foraminifera *Globigerinoides ruber* related to incursions of colder North Atlantic water into the Mediterranean Sea (Kandiano et al., 2014).

The influence of North Atlantic cold events on Mediterranean hydrology during the Early Last Glacial has been previously recognized in both the Sulmona and in the Corchia records (Regattieri et al., 2015; Drysdale et al., 2007). The occurrence of these events also in the POP record for the LIG thus confirms the linkage between high-latitude climate and Mediterranean hydrology under different climate boundary conditions (i.e.; glacials and interglacials), with cold/AMOC slowdown events in the North Atlantic triggering reduced precipitation in the Mediterranean. These findings also add to a growing number of paleoclimate records suggesting that large Northern Hemisphere ice sheets are not a fundamental prerequisite for triggering widespread millennial scale climate change. Instead, disruptions of the AMOC that are severe enough to cause drops in SSTs and associated water vapour advection and shifts in atmospheric circulation patterns in the North Atlantic, during full interglacial conditions, are seemingly capable of affecting the hydrology and environment of regions further downstream, such as the Mediterranean.

5.5 Conclusions

In this work we have presented a multiproxy record ($\delta^{13}\text{C}$, $\delta^{18}\text{O}$, elemental composition, and low-resolution biogenic silica and mineralogy) obtained from lacustrine sediments of the Sulmona Basin (central Italy). It is anchored to an independent time-scale based on tephrochronology, here improved by a new direct $^{40}\text{Ar}/^{39}\text{Ar}$ age (109.5 ± 0.9 ka, 2σ analytical uncertainty) for the widespread X-6 Mediterranean marker. Specifically, six tephra layers account for a relatively constant history of the sediment accumulation from ca. 129 ka to 92 ka, though chronological uncertainty is relatively high for the older interval investigated.

The resulting temporal series show prominent climatic and environmental changes on both long-term and millennial time-scale. Element concentrations and sediment mineralogy (quartz/calcite ratio from XRD analyses) show consistent patterns, with variations attributed to changes in the detrital clastic input to the lake. Lower detrital flux indicates reduced catchment erosion due to a denser vegetation cover and enhanced soil development under favourable climatic conditions, whereas enhanced mineral flux to the lake is related to events of climatic/environmental deterioration. $\delta^{18}\text{O}$ values are interpreted to reflect rainfall

amount in the high altitude catchment of the paleo-lake, with lower values indicating enhanced precipitation and possibly higher seasonality of the climate. Timing, amplitude, and general trends of the observed features are in agreement between the proxies indicating stronger catchment erosion (high detrital flux) during phases of lower precipitation (high $\delta^{18}\text{O}$). Our combined approach defines a clearer picture of environmental evolution during the observed period and confirms the hydrological significance of the $\delta^{18}\text{O}$ record from the Sulmona Basin, and more generally from the central Mediterranean continental carbonates.

Comparison between the Sulmona $\delta^{18}\text{O}$ record and speleothem $\delta^{18}\text{O}$ records located ~ 400 km to the north (Corchia and Tana che Urla Caves) shows consistent patterns down to the centennial time scale, and highlights several intra-interglacial events of reduced precipitation, which can be correlated among the three records within the associated uncertainty of each chronology. The most prominent is placed between 127.3 ka and 126.3 ka. Minor events of climate deterioration (lasting ~ 0.5 kyr) are apparent in all the continental $\delta^{18}\text{O}$ records at ca.123 ka, ca. 119 ka and ca. 116 ka, seem to have counterparts in a western Mediterranean faunal SST record, and possibly correspond to episodic phases of AMOC slowdown with episodic cold water-mass expansions and/or changes in the seasonal ice-sea cover in the North Atlantic. Overall, the new Sulmona record shows prominent intra-interglacial variability and suggests that North Atlantic SST variability during periods of low ice volume is capable of disrupting water ~~vapor~~vapour advection and atmospheric circulation patterns that feed Mediterranean hydrology.

Supplementary data to this article can be found online at <http://dx.doi.org/10.1016/j.palaeo.2017.02.013>.

Uncited references

~~Alpert et al., 2006~~

~~Eshel, 2002~~

Giraudi et al., 2011

~~Lionello et al., 2006~~

~~Lowe, 2011~~

North Greenland Ice Core Project Members, 2004

~~Oehlerich et al., 2013~~

~~Scholz and Hoffmann, 2014~~

~~Tzedakis, 2007~~

~~Wierzbowski, 2007~~

~~Wold et al., 2001~~

Acknowledgments

This work was funded by the Australian Research Council Discovery Project DP160102969 and by the University of Pisa through the project P.R.A. 2016 “Ruolo di zone di taglio nella costruzione degli orogeni: case histories da catene orogenetiche”. ER is supported by project SFB806 “Our way to Europe”. G. Zanchetta is thanked for discussion and comments to an early version of the manuscript. L. Folco is thanked for access to the HHXRF units, funded by the Italian “Ministero degli Affari Esteri e della Cooperazione Internazionale” (project ID#: PGR00187). D. Pecci, G. Luceretti and C. Gini are thanked for XRD data collection and R. Anis Ishak Nakhla is thanked for FESEM investigations. Two anonymous reviewers are also thanked for useful comments on the first version of the manuscript.

References

Alpert P., Baldi M., Ilani R., Krichak S., Price C., Rodo X. and Xoplaki E., Relations between climate variability in the Mediterranean region and the tropics: ENSO, South Asian and African monsoons, hurricanes and Saharan dust, *Dev. Earth Environ. Sci.* **4**, 2006, 149–177.

Barbieri M., Boschetti T., Petitta M. and Tallini M., Stable isotope (^2H , ^{18}O and $^{87}\text{Sr}/^{86}\text{Sr}$) and hydrochemistry monitoring for ground water ~~hydrodynamics~~ hydrodynamics analyses in a karst aquifer (Gran Sasso, Central Italy), *Applied Geochemistry* *Appl. Geochem.* **20**, 2005, 2063–2081.

- Bard E., Delaygue G., Rostek F., Antonioli F., Silenzi S. and Schrag D., Hydrological conditions in the western Mediterranean basin during the deposition of Sapropel 6 (ca. 175 kyr), *Earth Planet. Sci. Lett.* **202**, 2002, 481-494.
- Barker P., Telford R., Merdaci O., Williamson D., Taieb M., Vincens A. and Gibert E., The sensitivity of a Tanzanian crater lake to catastrophic tephra input and four millennia of climate change, *The Holocene* **10** (3), 2000, 303-310.
- Bar-Matthews M., Ayalon A. and Kaufmann A., Timing and hydrological conditions of Sapropel events in the eastern Mediterranean, as evident from speleothems, Soreq Cave, Israel, *Chemical Geology* *Chem. Geol.* **169**, 2000, 145-156.
- Bar-Matthews M., Ayalon A., Gilmor M., Matthews A. and Hawkesworth C.J., Sea-land oxygen isotopic relationships from planktonic foraminifera and speleothems in the Eastern Mediterranean region and their implication for paleorainfall during interglacial intervals, *Geochimica et Cosmochimica Acta* *Geochim. Cosmochim. Acta* **67**, 2003, 3181-3199.
- Bauch H.A., Kandiano E.S. and Helmke J.P., Contrasting ocean changes between the subpolar and polar North Atlantic during the past 135 ka, *Geophysical Research Letters* *Geophys. Res. Lett.* **39** (11), 2012.
- Berger A. and Loutre *M.-F.M.F.*, Insolation values for the climate of the last 10 million years, *Quaternary Science Reviews* *Quat. Sci. Rev.* **10** (4), 1991, 297-317.
- Blaauw M., Methods and code for 'classical' age-modelling of radiocarbon sequences, *Quat. Geochronol.* **5** (5), 2010, 512-518.
- Boch R., Cheng H., Spötl C., Edwards R.L. and Wang X., NALPS: a precisely dated European climate record 120-60 ka, *Climate of the Past* *Clim. Past* **7** (4), 2011, 1247-1259.
- Bourne A.J., Albert P.G., Matthews I.P., Trincardi F., Wulf S., Asioli A., Blockley S.P., Keller J. and Lowe J.J., Tephrochronology of core PRAD 1-2 in the Adriatic Sea: insights into Italian explosive volcanism for the period 200-80 ka, *Quaternary Science Reviews* *Quat. Sci. Rev.* **16**, 2015, 28-43.
- Brauer A., Allen J.R.M., Mingram J., Dulski P., Wulf S. and Huntley B., Evidence for the last interglacial chronology and environmental change from Southern Europe, *Proc. Natl. Acad. Sci. U. S. A.* **104**, 2007, 450-455.
- Brumsack H.-J., The trace metal content of recent organic carbon-rich sediments: implications for Cretaceous black shale formation, *Palaeogeography, Palaeoclimatology, Palaeoecology* *Palaeogeogr. Palaeoclimatol. Palaeoecol.* **232** (2-4), 2006, 344-361.
- Cacho I., Grimalt J.O., Sierro F.J., Shackleton N.J. and Canals M., Evidence of enhanced Mediterranean thermohaline circulation during the rapid climatic coolings, *Earth Planet. Sci. Lett.* **183**, 2000, 417-429.
- Cavinato G.P. and Miccadei E., Sintesi preliminare delle caratteristiche tettoniche e sedimentarie dei depositi quaternari della conca di Sulmona (L'Aquila), *Journal of Quaternary Science* *J. Quat. Sci.* **8**, 1995, 129-140.
- Cavinato *G.P.G.P.* and Miccadei E., Pleistocene carbonate lacustrine deposits: Sulmona basin (central Apennines, Italy), In: Gierlowsky-Kordesch *E.H.E.H.* and Kelts *K.R.K.R.*, (Eds.), *Lake Basins Through Space and Time, Studies in Geology, American Association of Petroleum Geologists* **46**, 2000, 517-526.
- Cavinato G.P., Cosentino D., De Rita D., Funicello R. and Parotto M., Tectonic sedimentary evolution of intrapenninic basins and correlation with the volcano-tectonic activity in central Italy, In: *Memorie Descrittive della Carta Geologica d'Italia* **49**, 1994, 63-76.
- Celle-jeanton H., Travi Y. and Blavoux B., Isotopic typology of the precipitation in the Western Mediterranean region at three different time scales, *Geophysical Research Letters* *Geophys. Res. Lett.* **28**, 2001, 1215-1218.
- Couchoud I., Genty D., Hoffmann D., Drysdale R.N. and Blamart D., Millennial-scale variability during the Last Interglacial recorded in a speleothem from south-western France, *Quaternary Science Reviews* *Quat. Sci. Rev.* **28**, 2009, 3263-3274.
- Curry *W.B.W.B.* and Oppo *D.W.D.W.*, Synchronous, high-frequency oscillations in tropical sea surface temperatures and North Atlantic Deep Water production during the last glacial cycle, *Paleoceanography* **12**, 1997, 1-14.
- Cvetkoska A., Levkov Z., Reed J.M., Wagner B., Panagiotopoulos K., Leng M.J. and Lacey J.H., Quaternary climate change and Heinrich events in the southern Balkans: Lake Prespa diatom palaeolimnology from the last interglacial to present, *Journal of Paleolimnology* *J. Paleolimnol.* **53** (2), 2015, 215-231.
- D.* Addabbo M., Sulpizio R., Guidi M., Capitani G., Mantecca P. and Zanchetta G., Ash leachates from some recent eruptions of Mount Etna (Italy) and Popocatepetl (Mexico) volcanoes and their impact on amphibian

living freshwater organisms, *Biogeosciences* **12**, 2015, 7087–7106.

Desiderio G., Rusi S. and Tatangelo F., Utilizzo di tecniche isotopiche (^{18}O e ^2H) nello studio delle acque sotterranee in aree protette dell'Appennino Abruzzese, *Riv. Ital. Agrometeorol.* **9** (1), 2005a, 90–91.

Desiderio G., Ferracuti L., Rusi S. and Tatangelo F., Il contributo degli isotopi naturali ^{18}O e ^2H nello studio delle idrostrutture carbonatiche abruzzesi e delle acque mineralizzate nell'area abruzzese e molisana, *Giorn. Geol. Appl.* **2**, 2005b, 453–458.

Development Core Team [R.R.](#), R: A Language and Environment for Statistical Computing, 2010, R Foundation for Statistical Computing; Vienna, Austria, (ISBN 3-900051-07-0).

Donato P., Albert P.G., Crocitti M., De Rosa R. and Menzies M.A., Tephra layers along the southern Tyrrhenian coast of Italy: Links to the X-5 & X-6 using volcanic glass geochemistry, *Journal of Volcanology and Geothermal Research / Volcanol. Geotherm. Res.* **317**, 2016, 30–41.

Drysdale R.N., Zanchetta G., Hellstrom J.C., Fallick A.E., Zhao J.X., Isola I. and Bruschi G., Palaeoclimatic implications of the growth history and stable isotope ($\delta^{18}\text{O}$ and $\delta^{13}\text{C}$) geochemistry of a Middle to Late Pleistocene stalagmite from central western Italy, *Earth and Planetary Science Letters / Earth Planet. Sci. Lett.* **227**, 2004, 215–229.

Drysdale [R.N.R.N.](#), Zanchetta G., Hellstrom J.C., Fallick A.E. and Zhao J.X., Stalagmite evidence for the onset of the Last Interglacial in southern Europe at 129 ± 1 ka, *Geophysical Research Letters / Geophys. Res. Lett.* **32**, 2005

Drysdale R.N., Zanchetta G., Hellstrom J.C., Maas R., Fallick A.E., Pickett M., Cartwright I. and Piccini L., Late Holocene drought responsible for the collapse of Old World civilizations is recorded in an Italian cave flowstone, *Geology* **34**, 2006, 101–104.

Drysdale R.N., Zanchetta G., Hellstrom J.C., Fallick A.E., McDonald J. and Cartwright I., Stalagmite evidence for the precise timing of North Atlantic cold events during the early last glacial, *Geology* **35**, 2007, 77–80.

Drysdale R.N., Hellstrom J.C., Zanchetta G., Fallick A.E., Sánchez Goñi M.F., Couchoud I., McDonald J., Maas R., Lohmann G. and Isola I., Evidence for Obliquity Forcing of Glacial Termination II, *Science* **325**, 2009, 1527–1531.

Eshel G., Mediterranean climates, *Israel Journal of Earth Sciences / Isr. J. Earth Sci.* **51**, 2002, 157–168.

Falcone [R.A.R.A.](#), Falgiani A., Parisse B., Petitta M., Spizzico M. and Tallini M., Chemical and isotopic ($\delta^{18}\text{O}$ ‰, $\delta^2\text{H}$ ‰, $\delta^{13}\text{C}$ ‰, ^{222}Rn) multi-tracing for groundwater conceptual model of carbonate aquifer (Gran Sasso INFN underground laboratory-central Italy), *Journal of Hydrology / J. Hydrol.* **357**, 2008, 368–388.

Francke A., Wagner B., Just J., Leicher N., Gromig R., Baumgarten H., Vogel H., Lacey J.H., Sadori L., Wonik T., Leng M.J., Zanchetta G., Sulpizio R. and Giaccio B., Sedimentological processes and environmental variability at Lake Ohrid (Macedonia, Albania) between 637 ka and the present, *Biogeosciences* **13** (4), 2016, 1179–1196.

Freytet P. and Verrecchia E.P., Lacustrine and palustrine carbonate petrography: an overview, *Journal of Paleolimnology / J. Paleolimnol.* **27** (2), 2002, 221–237.

Galaasen E.V., Ninnemann U.S., Irvah N., Kleiven H.K.F., Rosenthal Y., Kissel C. and Hodell D.A., Rapid reductions in North Atlantic Deep Water during the peak of the last interglacial period, *Science* **343** (6175), 2014, 1129–1132.

Galli P., Giaccio B., Peronace E. and Messina P., Holocene paleoearthquakes and Early-Late Pleistocene slip-rate on the Sulmona Fault (Central Apennines, Italy), *Bulletin of the Seismological Society of America / Bull. Seismol. Soc. Am.* **105**, 2015, 1–13.

Gemelli M., D'Orazio M. and Folco L., Chemical Analysis of Iron Meteorites Using a Hand-Held X-Ray Fluorescence Spectrometer, *Geostandards and Geoanalytical Research / Geostand. Geoanal. Res.* **39** (1), 2015, 55–69.

Giaccio B., Messina P., Sposato A., Voltaggio M., Zanchetta G., Galadini F., Gori S. and Santacroce R., Tephra layers from Holocene lake sediments of the Sulmona Basin, central Italy: implications for volcanic activity in Peninsular Italy and tephrostratigraphy in the central Mediterranean area, *Quaternary Science Reviews / Quat. Sci. Rev.* **28** (25), 2009, 2710–2733.

Giaccio B., Nomade N., Wulf S., Isaia R., Sottili G., Cavuoto G., Galli P., Messina P., Sposato A., Sulpizio R. and Zanchetta G., The late MIS 5 Mediterranean tephra markers: a reappraisal from peninsular Italy terrestrial records, *Quaternary Science Reviews / Quat. Sci. Rev.* **56**, 2012, 31–45.

Giaccio B., Castorina F., Nomade S., Scardia G., Voltaggio M. and Sagnotti L., Revised chronology of the Sulmona lacustrine succession, central Italy, *Journal of Quaternary Science / J. Quat. Sci.* **28**, 2013a, 545–551.

- Giaccio B., Arienzo I., Sottili G., Castorina F., Gaeta M., Nomade S., Galli P. and Messina P., Isotopic (Sr-Nd) and major element fingerprinting of distal tephras: an application to the Middle-Late Pleistocene markers from the Colli Albani volcano, central Italy, *Quaternary Science Reviews* *Quat. Sci. Rev.* **67**, 2013b, 190-206.
- Giaccio B., Regattieri E., Zanchetta G., Nomade S., Renne P.R., Sprain C.J., Drysdale R.N., Tzedakis P.C., Messina P., Scardia G., Sposato A. and Bassinot F., Duration and dynamics of the best orbital analogue to the present interglacial, *Geology* **43** (7), 2015a, 603-606.
- Giaccio B., Regattieri E., Zanchetta G., Wagner B., Galli P., Mannella G., Niespolo E., Peronace E., Renne P., Nomade S., Cavinato G.P., Messina P., Sposato A., Boschi C., Florindo F., Marra F. and Sadori L., A key continental archive for the last 2 Ma of climatic history in central Mediterranean area: a preliminary report on the Fucino deep-drilling project, central Italy, *Scientific Drilling* *Sci. Drill.* **3**, 2015b, 1-7 (Giaccio B., Niespolo E., Pereira A., Nomade S., Renne P., Albert G.P., Arienzo I., Regattieri E., Wagner B., Zanchetta G., Gaeta M., Galli P., Mannella G., Peronace E., Sottili G., Florindo F., Leicher N., Marra F., Tomlinson E.L. First integrated tephrochronological record for the last ~190 kyr from the Fucino Quaternary lacustrine succession, central Italy. *Quat. Sci. Rev.* **158**, 2017, 211-234).
- Gierlowsky-Kordesch E.H., Lacustrine eCarbonates, In: *Developments in Sedimentology* **61**, 2010, 2-50.
- Giraudi C., Magny M., Zanchetta G. and Drysdale R.N., The Holocene climatic evolution of the Mediterranean Italy: a review of the geological continental data, *The Holocene* **21**, 2011, 105-115.
- Giraudi C., Zanchetta G. and Sulpizio R., A Late-Pleistocene phase of Saharian dust deposition in the high Apennine mountains (Italy), *Alpine Mediterr. Quat.* **26**, 2013, 110-122.
- Govin A., Capron E., Tzedakis P.C., Verheyden S., Ghaleb B., Hillaire-Marcel C., St-Onge G., Stoner J.S., Bassinot F., Bazin L., Blunier T., Combourieu-Nebout N., El Ouahabi A., Genty D., Gersonde R., Jimenez-Amat P., Landais A., Martrat B., Masson-Delmotte V., Parrenin F., Seidenkrantz M.S., Veres D., Waelbroeck C. and Zahn R., Sequence of events from the onset to the demise of the Last Interglacial: Evaluating strengths and limitations of chronologies used in climatic archives, *Quaternary Science Reviews* *Quat. Sci. Rev.* **129**, 2015, 1-36.
- Hollander D.J. and McKenzie J.A., CO₂ control on carbon-isotope fractionation during aqueous photosynthesis: a paleo-pCO₂ barometer, *Geology* **19**, 1991, 929-932.
- Insinga D.D., Tamburrino S., Lirer F., Vezzoli L., Barra M., De Lange G.J., Tiepolo M., Vallefucio M., Mazzola S. and Sprovieri M., Tephrochronology of the astronomically-tuned KC01B deep-sea core, Ionian Sea: Insights into the explosive activity of the Central Mediterranean area during the last 200 ka, *Quaternary Science Reviews* *Quat. Sci. Rev.* **85**, 2014, 63-84.
- Iorio M., Liddicoat J., Budillon F., Incoronato A., Coe R.S., Insinga D., Cassata W., Lubritto C., Angelino A. and Tamburrino S., Combined palaeomagnetic secular variation and petrophysical records to time constrain geological and hazardous events: an example from the eastern Tyrrhenian Sea over the last 120 ka, *Glob. Planet. Chang.* **113**, 2014, 91-109.
- Irvali N., Ninnemann U.S., Galaasen E.V., Rosenthal Y., Kroon D., Oppo D.W., Kleiven H.F., Darling K.F. and Kissel C., Rapid switches in subpolar North Atlantic hydrography and climate during the Last Interglacial (MIS 5e), *Paleoceanography* **27** (2), 2012, PA2207.
- Johnson F.C.T.C., Brown E.T.E.T. and Shi J., Biogenic silica deposition in Lake Malawi, East Africa over the past 150,000 years, *Palaeogeography, Palaeoclimatology, Palaeoecology* *Palaeogeogr. Palaeoclimatol. Palaeoecol.* **303** (1), 2011, 103-109.
- Jovanovska E., Cvetkoska A., Hauffe T., Levkov Z., Wagner B., Sulpizio R., Francke A., Albrecht C. and Wilke T., Differential resilience of ancient sister lakes Ohrid and Prespa to environmental disturbances during the Late Pleistocene, *Biogeosciences* **13** (4), 2016, 1149-1161.
- Kandiano E.S., Bauch H.A. and Fahl K., Last interglacial surface water structure in the western Mediterranean (Balearic) Sea: Climatic variability and link between low and high latitudes, *Global and Planetary Change* *Glob. Planet. Chang.* **123**, 2014, 67-76.
- Keller J., Ryan W.B.F., Ninkovich D. and Altherr R., Explosive volcanic activity in the Mediterranean over the past 200,000 years as recorded in deep-sea sediments, *Geological Society of America Bulletin* *Geol. Soc. Am. Bull.* **89**, 1978, 591-604.
- Kelts K. and Hsü K.J., Freshwater carbonate sedimentation, In: Lerman A.A. (Ed), *Lakes, Chemistry, Geology, Physics*, 1978, Springer-Verlag; Berlin, 295-323.
- Kelts K. and Talbot M., Lacustrine carbonates as geochemical archives of environmental change and biotic/abiotic interactions, In: *Large Lakes*, 1990, Springer Berlin Heidelberg, 288-315.
- Kim S.T. and O'Neil J.R., Equilibrium and nonequilibrium oxygen isotope effects in synthetic carbonates, *Geochimica et Cosmochimica Acta* *Geochim. Cosmochim. Acta* **61** (16), 1997, 3461-3475.

- Koinig K.A., Shotyk W., Lotter A.F., Ohlendorf C. and Sturm M., 9000 years of geochemical evolution of lithogenic major and trace elements in the sediment of an alpine lake - the role of climate, vegetation and land-use history, *Journal of Paleolimnology* **30**, 2003, 307-320.
- Kukla G.-J.G.J., Bender M.-L.M.L., de Beaulieu J.-L.J.L., Bond G., Broecker W.-S.W.S., Cleveringa P., Gavin J.E., Herbert T.D., Imbrie J., Jouzel J., Keigwin L.-D.L.D., Knudsen K.-L.K.-L., McManus J., Merkt J., Muhs D.R., Muller H., Poore R.Z. and Porter S.C., Last Interglacial Climates, *Quaternary Research* **58** (1), 2002, 2-13.
- Kylander M.E., Ampel L., Wohlfarth B. and Veres D., High-resolution X-ray fluorescence core scanning analysis of Les Echets (France) sedimentary sequence: new insights from chemical proxies, *Journal of Quaternary Sciences* **26** (1), 2011, 109-117.
- Kylander M.E., Klaminder J., Wohlfarth B. and Löwemark L., Geochemical responses to paleoclimatic changes in southern Sweden since the late glacial: the Hässeldala Port lake sediment record, *Journal of Paleolimnology* **50** (1), 2013, 57-70.
- Leicher N., Zanchetta G., Sulpizio R., Giaccio B., Wagner B., Nomade S., Francke A. and Del Carlo P., First tephrostratigraphic results of the DEEP site record from Lake Ohrid (Macedonia and Albania), *Biogeosciences* **13**, 2016, 2151-2178.
- Leng M.J. and Marshall J.D., Palaeoclimate interpretation of stable isotope data from lake sediment archives, *Quaternary Science Reviews* **23**, 2004, 811-831.
- Leng M.-J.M.J., Jones M.-D.M.D., Frogley M.-R.M.R., Eastwood W.-J.W.J., Kendrick C.-P.C.P. and Roberts C.-N.C.N., Detrital carbonate influences on bulk oxygen and carbon isotope composition of lacustrine sediments from the Mediterranean, *Global and Planetary Change* **71** (3), 2010, 175-182.
- Lézine A.M., von Grafenstein U., Andersen N., Belmecheri S., Bordon A., Caron B., Cazet P., Erlenkeuser H., Fouache E., Grenier C., Huntsman-Mapila P., Hureau-Mazaudier D., Manelli D., Mazaud A., Robert C., Sulpizio R., Tiercelin J.J., Zanchetta G. and Zeqollari Z., Lake Ohrid, Albania, provides an exceptional multi-proxy record of environmental changes during the last glacial-interglacial cycle, *Palaeogeography, Palaeoclimatology, Palaeoecology* **287**, 2010, 116-127.
- Lionello P., Bhend J., Buzzi A., Della-Marta P.M., Krichak S., Jansà A., Maheras P., Sanna A., Trigo I.F. and Trigo R., Cyclones in the Mediterranean region: climatology and effects on the environment, In: Lionello P., Malanotte-Rizzoli P. and Boscolo R., (Eds.), *Mediterranean Climate Variability*, 2006, Elsevier (NETHERLANDS); Amsterdam, (324-372).
- Longinelli A. and Selmo E., Isotopic composition of precipitation in Italy: a first overall map, *Journal of Hydrology* **270**, 2003, 75-88.
- Longinelli A., Anglesio E., Flora O., Iacumin P. and Selmo E., Isotopic composition of precipitation in Northern Italy: reverse effect of anomalous climatic events, *Journal of Hydrology* **329** (3), 2006, 471-476.
- Lowe D.-J.D.J., Tephrochronology and its application: a review, *Quaternary Geochronology* **6** (2), 2011, 107-153.
- Löwemark L., Chen H.F., Yang T.-N.T.N., Kylander M.E., Yu E.F., Hsu Y.W., Lee T.Q., Song S.R. and Jarvis S., Normalizing XRF-scanner data: a cautionary note on the interpretation of high-resolution records from organic-rich lakes, *Journal of Asian Earth Sciences* **40**, 2011, 1250-1256.
- Marino G., Rohling E.J., Rodríguez-Sanz L., Grant K.M., Heslop D., Roberts A.P., Stanford J.D. and Yu J., Bipolar seesaw control on last interglacial sea level, *Nature* **522** (7555), 2015, 197-201.
- Martrat B., Grimalt J.O., Lopez-Martinez C., Chaco I., Sierro F.J., Flores J.A., Zahn R., Canals M., Jason H.C. and Hodell D.A., Abrupt temperature changes in the Western Mediterranean over the past 250,000 years, *Science* **306**, 2004, 1762-1765.
- Martrat B., Jimenez-Amat P., Zahn R. and Grimalt J.-O.J.O., Similarities and dissimilarities between the last two deglaciations and interglaciations in the North Atlantic region, *Quaternary Science Reviews* **99**, 2014, 122-134.
- Mayer B. and Schwark L., A 15,000-year stable isotope record from sediments of Lake Steisslingen, Southwest Germany, *Chemical Geology* **161**, 1999, 315-337.
- McManus J., Bond G., Broecker W., Johnsen S., Labeyrie L. and Higgins S., High-resolution climate records from the North Atlantic during the Last Interglacial, *Nature* **371**, 1994, 326-329.
- Meyer-Jacob C., Vogel H., Boxberg F., Rosén P., Weber M.E. and Bindler R., Independent measurement of biogenic silica in sediments by FTIR spectroscopy and PLS regression, *Journal of Paleolimnology*

Paleolimnol **52**, 2014, 245-255.

Miccadei E., Barberi R. and Cavinato G.P., La geologia quaternaria della conca di Sulmona (Abruzzo, Italia centrale), *Geologica Romana Geol. Romana* **34**, 1998, 59-86.

Milner *A.-M.A.M.*, Collier *R.-E.R.E.*, Roucoux *K.-H.K.H.*, Müller *U.-C.U.C.*, Pross J., Kalaitzidis S. and Tzedakis *P.-C.P.C.*, Enhanced seasonality of precipitation in the Mediterranean during the early part of the Last Interglacial, *Geology* **40**, 2012, 919-922.

Milner *A.-M.A.M.*, Müller *U.-C.U.C.*, Roucoux *K.-H.K.H.*, Collier *R.-E.R.E.*, Pross J., Kalaitzidis S. and Tzedakis *P.-C.P.C.*, Environmental variability during the Last Interglacial: a new high-resolution pollen record from Tenaghi Philippon, Greece, *Journal of Quaternary Science J. Quat. Sci.* **28** (2), 2013, 113-117.

Milner *A.-M.A.M.*, Roucoux *K.-H.K.H.*, Collier *R.-E.-L.R.E.L.*, Müller *U.-C.U.C.*, Pross J. and Tzedakis *P.-C.P.C.*, Vegetation responses to abrupt climatic changes during the Last Interglacial Complex (Marine Isotope Stage 5) at Tenaghi Philippon, NE Greece, *Quaternary Science Reviews Quat. Sci. Rev.* **154**, 2016, 169-181.

Mook W.G. and Tan F.C., Stable carbon isotopes in rivers and estuaries, In: Degens *F.F.E.T.*, Kempe *S.S.* and Richey *F.E.* (Eds.), *Biogeochemistry of Major World Rivers*, 1991, John Wiley; New York, 245-264.

Narcisi B., Late Quaternary eolian deposition in central Italy, *Quaternary Research Quat. Res.* **54** (2), 2000, 246-252.

Nomade S., Renne P.R., Vogel N., Deino A.L., Sharp W.D., Becker T.A., Jaouni A.R. and Mundil R., Alder Creek sanidine (ACs-2): a Quaternary $^{40}\text{Ar}/^{39}\text{Ar}$ dating standard tied to the Cobb Mountain geomagnetic event, *Chemical Geology Chem. Geol.* **218**, 2005, 315-338.

Nomade S., Gauthier A., Guillou H. and Pastre J.F., $^{40}\text{Ar}/^{39}\text{Ar}$ temporal framework for the Alleret maar lacustrine sequence (French Massif-Central): volcanological and paleoclimatic implications, *Quaternary Geochronology Quat. Geochronol.* **5**, 2010, 20-27.

North Greenland Ice Core Project Members, High-resolution record of Northern Hemisphere climate extending into the last interglacial period, *Nature* **431**, 2004, 147-151.

Oehlerich M., Baumer M., Lücke A. and Mayr C., Effects of organic matter on carbonate stable isotope ratios ($\delta^{13}\text{C}$, $\delta^{18}\text{O}$ values)-implications for analyses of bulk sediments, *Rapid Communications in Mass Spectrometry Rapid Commun. Mass Spectrom.* **27**, 2013, 707-712.

Oppo D.W., Keigwin L.D. and McManus J.F., Persistent suborbital climate variability in marine isotope stage 5 and Termination II, *Paleoceanography* **16**, 2001, 280-292.

Oppo D.W., McManus J.F. and Cullen J.L., Evolution and demise of the Last Interglacial warmth in the subpolar North Atlantic, *Quaternary Science Reviews Quat. Sci. Rev.* **25**, 2006, 3268-3277.

Paterne M., Guichard F., Duplessy J.C., Siani G., Sulpizio R. and Labeyrie J., A 90,000-200,000 years marine tephra record of Italian volcanic activity in the Central Mediterranean Sea, *Journal of Volcanology and Geothermal Research J. Volcanol. Geotherm. Res.* **177**, 2008, 187-196.

Petrosino P., Morabito S., Jicha *B.-R.B.R.*, Milia A., Sprovieri M. and Tamburrino S., Multidisciplinary tephrochronological correlation of marker events in the eastern Tyrrhenian Sea between 48 and 105 ka, *Journal of Volcanology and Geothermal Research J. Volcanol. Geotherm. Res.* **315**, 2016, 79-99.

Pol K., Masson-Delmotte V., Cattani O., Debret M., Falourd S., Jouzel J., Landais A., Minster B., Mudelsee M., Schulz M. and Stenni B., Climate variability features of the last interglacial in the East Antarctic EPICA Dome C ice core, *Geophysical Research Letters Geophys. Res. Lett.* **41** (11), 2014, 4004-4012.

Prokopenko A.A., Hinnov L.A., Williams D.F. and Kuzmin M.I., Orbital forcing of continental climate during the Pleistocene: a complete astronomically tuned climatic record from Lake Baikal, SE Siberia, *Quaternary Science Reviews Quat. Sci. Rev.* **25**, 2006, 3431-3457.

Rasmussen *F.-L.T.L.*, Thomsen E., Labeyrie L. and van Weering *F.-C.T.C.*, Circulation changes in the Faeroe-Shetland Channel correlating with cold events during the last glacial period (58-10 ka), *Geology* **24**, 1996, 937-940.

Regattieri E., Isola I., Zanchetta G., Drysdale R.N., Hellstrom J.C. and Baneschi I., Stratigraphy, petrography and chronology of speleothem concretion at Tana Che Urla (Lucca, Italy): paleoclimatic implications, *Geogr. Fis. Dinamica Quat.* **35**, 2012, 141-152.

- Regattieri E., Zanchetta G., Drysdale R.N., Isola I. and Roncioni A., A continuous stable isotopic record from the Penultimate glacial maximum to the Last Interglacial (159 to 121 ka) from Tana Che Urla Cave (Apuan Alps, central Italy), *Quaternary Research* *Quat. Res.* **82**, 2014a, 450-461.
- Regattieri E., Zanchetta G., Drysdale R., Isola I., Hellstrom J. and Dallai L., Lateglacial to Holocene trace element record (Ba, Mg, Sr) from Corchia Cave (Apuan Alps, central Italy): paleoenvironmental implications, *Journal of Quaternary Science* *J. Quat. Sci.* **29** (4), 2014b, 381-392.
- Regattieri E., Giaccio B., Zanchetta G., Drysdale R.N., Galli P., Nomade S., Peronace E. and Wulf S., Hydrological variability over the Apennines during the Early Last Glacial precession minimum, as revealed by a stable isotope record from Sulmona basin, Central Italy, *Journal of Quaternary Science* *J. Quat. Sci.* **30** (1), 2015, 19-31.
- Regattieri E., Zanchetta G., Drysdale R.N., Woodhead J.D., Hellstrom J., Giaccio B., Isola I., Greig A. and Banerjee, Environmental variability between the penultimate deglaciation and the mid Eemian: insights from Tana che Urla (central Italy) speleothem trace element record, *Quaternary Science Reviews* *Quat. Sci. Rev.* **152**, 2016a, 80-92.
- Regattieri E., Giaccio B., Galli P., Nomade S., Peronace E., Messina P., Sposato A., Boschi C. and Gemelli M., A multi-proxy record of MIS 11-12 deglaciation and glacial MIS 12 instability from the Sulmona Basin (central Italy), *Quaternary Science Reviews* *Quat. Sci. Rev.* **32**, 2016b, 129-145.
- Roberts N., Jones M.D., Benkaddur A., Eastwood W.J., Filippi M.L., Frogley M.R., Lamb H.F., Leng M.J., Reed J.M., Stein M., Stevens L., Valero-Garcè B. and Zanchetta G., Stable isotope records of Late Quaternary climate and hydrology from Mediterranean lakes: the ISOMED synthesis, *Quat. Sci. Rev.* **27**, 2008, 2426-2441.
- Rohling E.J., Marino G. and Grant K.M., Mediterranean climate and oceanography, and the periodic development of anoxic events (sapropels), *Earth Science Reviews* *Earth-Sci. Rev.* **143**, 2015, 62-97.
- Rosén P., Vogel H., Cunningham L., Reuss N., Conley D.-J.D.J. and Persson P., Fourier transform infrared spectroscopy, a new method for rapid determination of total organic and inorganic carbon and biogenic silica concentration in lake sediments, *Journal of Paleolimnology* *J. Paleolimnol.* **43** (2), 2010, 247-259.
- Russo-Ermolli E., Aucelli P.P., Di Rollo A., Mattei M., Petrosino P., Porreca M. and Rosskopf C.M., An integrated stratigraphical approach to the Middle Pleistocene succession of the Sessano basin (Molise, Italy), *Quaternary International* *Quat. Int.* **225** (1), 2010, 114-127.
- Sadori L., Koutsodendris A., Masi A., Bertini A., Combourieu-Nebout N., Francke A., Kouli K., Joannin S., Mercuri A.M., Peyron O., Torri P., Wagner B., Zanchetta G., Sinopoli G. and Donders T.H., Pollen-based paleoenvironmental and paleoclimatic change at Lake Ohrid (SE Europe) during the past 500 ka, *Biogeosciences* **13**, 2016, 1423-1437.
- Sagnotti L., Scardia G., Giaccio B., Liddicoat J.C., Nomade S., Renne P.R. and Sprain C.J., Extremely rapid directional change during Matuyama-Brunhes geomagnetic polarity reversal, *Geophysical Journal International* *Geophys. J. Int.* **199**, 2014, 1110-1124.
- Sagnotti L., Giaccio B., Liddicoat J.-G.J.C., Nomade S., Renne P.-R.P.R., Scardia G. and Sprain C.-J.C.J., How fast was the Matuyama-Brunhes geomagnetic reversal? A new subcentennial record from the Sulmona Basin, central Italy, *Geophysical Journal International* *Geophys. J. Int.* **204** (2), 2016, 798-812.
- Sánchez-Goñi M.F., Eynaud F., Turon J.-L.J.L. and Shackleton N.-J.N.J., High resolution palynological record off the Iberian margin: direct land-sea correlation for the Last Interglacial complex, *Earth and Planetary Science Letters* *Earth Planet. Sci. Lett.* **171** (1), 1999, 123-137.
- Schnetger B., Brumsack H.J., Schale H., Hinrichs J. and Dittert L., Geochemical characteristics of deep-sea sediments from the Arabian Sea: a high-resolution study, *Deep-Sea Res. II* **47**, 2000, 2735-2768.
- Scholz D. and Hoffmann D.L., StalAge - An algorithm designed for construction of speleothem age models, *Quaternary Geochronology* *Quat. Geochronol.* **6**, 2011, 369-382.
- Seelos K. and Sirocko F., Abrupt Cooling Events at the Very End of the Last Interglacial. The climate of the past interglacial, *Dev. Quat. Sci.* **7**, 2007, 207-229.
- Seelos K., Sirocko F. and Dietrich S., A continuous high-resolution dust record for the reconstruction of wind systems in central Europe (Eifel, Western Germany) over the past 133 ka, *Geophysical Research Letters* *Geophys. Res. Lett.* **36** (20), 2009.
- Sirocko F., Seelos K., Schaber K., Rein B., Dreher F., Diehl M., Lehne R., Jäger K., Krbetschek M. and Degering D., A late Eemian aridity pulse in central Europe during the last glacial inception, *Nature* **436**, 2005, 833-836.

- Sprovieri R., Di Stefano E., Incarbona A. and Oppo [D.-W.D.W.](#), Suborbital climate variability during Marine Isotopic Stage 5 in the central Mediterranean basin: evidence from calcareous plankton record, [Quaternary Science Reviews](#) *Quat. Sci. Rev.* **25** (17), 2006, 2332-2342.
- Sulpizio R., Zanchetta G., D'Orazio M., Vogel H. and Wagner B., Tephrostratigraphy and tephrochronology of lakes Ohrid and Prespa, Balkans, *Biogeosciences* **7**, 2010, 3273-3288.
- Talbot M.R., A review of the palaeohydrological interpretation of carbon and oxygen isotopic ratios in primary lacustrine carbonates, *Chem. Geol. Isot. Geosci. Sect.* **80** (4), 1990, 261-279.
- Toucanne S., Minto'o [C.-M.A.C.M.A.](#), Fontanier C., Bassetti [M.-A.M.A.](#), Jorriy [S.-J.S.J.](#) and Jouet G., Tracking rainfall in the northern Mediterranean borderlands during sapropel deposition, [Quaternary Science Reviews](#) *Quat. Sci. Rev.* **129**, 2015, 178-195.
- Tzedakis P.C., Seven ambiguities in the Mediterranean palaeoenvironmental narrative, [Quaternary Science Reviews](#) *Quat. Sci. Rev.* **26**, 2007, 2042-2066.
- Tzedakis [P.-C.P.C.](#), Frogley [M.-R.M.R.](#) and Heaton [T.-H.E.T.H.E.](#), Last Interglacial conditions in southern Europe: evidence from Ioannina, northwest Greece, [Global and Planetary Change](#) *Glob. Planet. Chang.* **36** (3), 2003, 157-170.
- Vidal L., Labeyrie L., Cortijo E., Arnold M., Duplessy [J.-C.J.C.](#), Michel E. and Van Weering [F.-C.-E.T.C.E.](#), Evidence for changes in the North Atlantic Deep Water linked to meltwater surges during the Heinrich events, [Earth and Planetary Science Letters](#) *Earth Planet. Sci. Lett.* **146**, 1997, 13-27.
- Villa V., Pereira A., Chaussé C., Nomade S., Giaccio B., Limondin-Lozouet N., Fusco F., Regattieri E., Degeai J.P., Robert V., Kuzucuoglu C., Boschian G., Aureli D., Pagli M., Bahain J.J. and Nicoud E., A MIS 15-MIS 12 record of environmental changes and Lower Palaeolithic occupation from Valle Giumentina, central Italy, [Quaternary Science Reviews](#) *Quat. Sci. Rev.* **151**, 2016, 160-184.
- Vogel H., Rosén P., Wagner B., Melles M. and Persson P., Fourier transform infrared spectroscopy, a new cost-effective tool for quantitative analysis of biogeochemical properties in long sediment records, [Journal of Paleolimnology](#) *J. Paleolimnol.* **40** (2), 2008, 689-702.
- Vogel H., Wagner B., Zanchetta G., Sulpizio R. and Rosén P., A paleoclimatic record with tephrochronological age control for the last glacial-interglacial cycle from Lake Ohrid, Albania and Macedonia, [Journal of Paleolimnology](#) *J. Paleolimnol.* **44**, 2010, 295-310.
- Vogel H., Meyer-Jacob C., Thöle L., Lippold J.A. and Jaccard S.L., Quantification of biogenic silica by means of Fourier transform infrared spectroscopy (FTIRS) in marine sediments, *Limnol. Oceanogr. Methods* 2016, <http://dx.doi.org/10.1002/lom3.10129>, (in press).
- Wehausen R. and Brumsack H.J., Cyclic variations in the chemical composition of eastern Mediterranean Pliocene sediments: a key for understanding sapropel formation, [Marine Geology](#) *Mar. Geol.* **153** (1-4), 1999, 161-176.
- Wierzbowski H., Effects of pre-treatments and organic matter on oxygen and carbon isotope analyses of skeletal and inorganic calcium carbonate, [International Journal of Mass Spectrometry](#) *Int. J. Mass Spectrom.* **268**, 2007, 16-29.
- Wold S., Sjöström M. and Eriksson L., PLS-regression: a basic tool of chemometrics, [Chemometrics and intelligent laboratory systems](#) *Chemom. Intell. Lab. Syst.* **58** (2), 2001, 109-130.
- Wulf S., Keller J., Paterne M., Mingram J., Lauterbach S., Opitz S., Sottili G., Giaccio B., Albert P., Satow C., Viccaro M. and Brauer A., The 100-133 record of Italian explosive volcanism and revised tephrochronology of Lago Grande di Monticchio, [Quaternary Science Reviews](#) *Quat. Sci. Rev.* **58**, 2012, 104-123.
- Yancheva G., Nowaczyk N.R., Mingram J., Dulski P., Schettler G., Negendank J.F.W., Liu J., Sigman D.M., Peterson L.C. and Haug G.H., Influence of the intertropical convergence zone on the East Asian monsoon, *Nature* **445** (7123), 2007, 74-77.
- Zanchetta G., Bonadonna F.P. and Leone G., A 37-meter record of paleoclimatological events from stable isotope data on molluscs in Valle di Castiglione, near Rome, Italy, [Quaternary Research](#) *Quat. Res.* **52**, 1999, 293-299.
- Zanchetta G., Drysdale R.N., Hellstrom J.C., Fallick A.E., Isola I., Gagan M. and Pareschi M.T., Enhanced rainfall in the western Mediterranean during deposition of Sapropel S1: stalagmite evidence from Corchia Cave (Central Italy), *Quat. Sci. Rev.* **26**, 2007a, 279-286.

Zanchetta G., Borghini A., Fallick A.E., Bonadonna F.P. and Leone G., Late Quaternary palaeohydrology of Lake Pergusa (Sicily, southern Italy) as inferred by stable isotopes of lacustrine carbonates, *Journal of Paleolimnology* **38**, 2007b, 227-239.

Zanchetta G., van Welden A., Baneschi I., Drysdale R.N., Sadori L., Roberts N., Giardini M., Beck C., Pascucci V. and Sulpizio R., Multiproxy record for the last 4500 years from Lake Shkodra (Albania/Montenegro), *Journal of Quaternary Science* **27**, 2012, 780-789.

Zanchetta G., Bar-Matthews M., Drysdale R.N., Lionello P., Ayalon A., Hellstrom J.C., Isola I. and Regattieri E., Coeval dry events in the central and eastern Mediterranean basin at 5.2 and 5.6 ka recorded in Corchia (Italy) and Soreq caves (Israel) speleothems, *Global and Planetary Change* **122** (2014), 2014, 130-139.

Zanchetta G., Regattieri E., Isola I., Drysdale R.N., Bini M., Baneschi I. and Hellstrom J.C., The so-called "4.2 event" in the central Mediterranean and its climatic teleconnections, *Alpine Mediterr. Quat.* **29** (1), 2016 **2016a**, 5-17.

Zanchetta G., Regattieri E., Giaccio B., Wagner B., Sulpizio R., Francke A., Vogel L.H., Sadori L., Masi A., Sinopoli G., Lacey J.H., Leng M.L. and Leicher N., Aligning MIS5 proxy records from Lake Ohrid (FYROM) with independently dated Mediterranean archives: implications for core chronology, *Biogosciences* **13** (9), **2016a** **2016b**, 2757-2768.

▼ E-Extra

Full analytical details for the 13 individual crystals analyses are given in [Supplementary Table S1](#). Age-probability density spectra with individual single crystal age are presented [Fig. 3](#). Among the 13 crystals analysed, ten yielded a similar age. These juvenile crystals allowed calculation of a weighted mean age of 109.5 ± 0.9 ka (2σ analytical uncertainty, $P = 0.94$).

The depth and temporal series of the analysed elements (Ti, Rb, Zr, Al, Si, Ca, Sr) are shown in [Figs. 2 and 6](#), respectively. Correlation coefficients are reported in [Table 2](#) while scatterplots are reported in supplementary [Fig. S1](#).

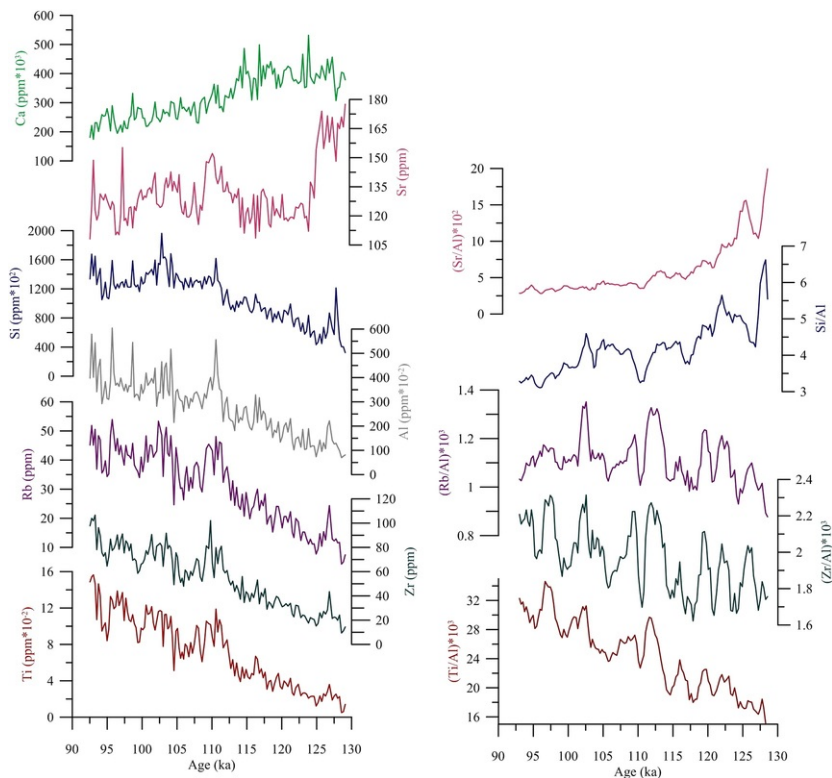


Fig. 6 Left panel: XRF results plotted vs. age (from bottom: Ti, Zr, Rb, Al, Si, Sr, Ca); right panel: Five-point smoothed time series of normalized XRF data (from bottom: Ti/Al, Zr/Al, Rb/Al, Si/Al, Sr/Al).

alt-text: Fig. 6

Table 2 Pearson correlation coefficients (r) between elements concentration (XRF data, $n = 141$)

alt-text: Table 2

	Ca					
Sr	+ 0.17	Sr				
Ti	0.85	0.29	Ti			
Zr	0.85	0.25	+ 0.98	Zr		
Rb	0.79	0.27	+ 0.96	+ 0.97	Rb	
Si	0.67	0.35	+ 0.86	+ 0.86	+ 0.90	Si
Al	0.65	0.29	+ 0.91	+ 0.89	+ 0.93	+ 0.92

An approach which is traditionally used to overcome the dilution effect is the normalization of element concentrations by a conservative, lithogenic element (e.g. [Kylander et al., 2011, 2013](#) [Löwemark et al., 2011](#); [Vogel et al., 2010](#)). In many cases, normalization allows one to identify misleading trends in element concentrations. The element to be used for normalization should not itself be a proxy nor be affected by biological or redox processes ([Löwemark et al., 2011](#)). Ti is widely used for normalization as it is a common accessory component in various mineral phases and is conservative in terms of its reactivity. However, Ti is

enriched in heavy minerals and in aeolian dust, and in particular settings it can therefore be used as a proxy for high-current regimes (Schnetger et al., 2000) or enhanced wind activity (Wehausen and Brumsack, 1999; Yancheva et al., 2007). Another element suitable for normalization is Al (Löwemark et al., 2011), which is a major component of siliciclastic mineral phases and, similar to Ti, is not significantly affected by redox and biologically mediated reactions (Brumsack, 2006). Once this approach is applied to our XRF series, the correlation coefficients between Zr/Al, Ti/Al and Rb/Al, which are exclusively of detrital origin, remain high (Table 2, Fig. S2), and the increasing long-term trend in element ratios compares well with element concentrations from ca. 129 ka to 92 ka (Fig. 6). Thus, normalization using Al confirms the exclusively detrital origin for Zr, Ti and Rb, and that the observed long-term trends are not an artefact caused by CaCO₃ dilution. Specifically, all three ratios show a twofold structure, with an older (up to ca. 115 ka) part displaying a lower clastic input and a younger part (90–115 ka) with a higher sediment delivery. They also show clear maxima at ca. 111 ka and 103 ka, corresponding to periods of higher $\delta^{18}\text{O}$ values, which we interpret as indication of drier conditions.

▼ E-component

The following are the supplementary data related to this article.

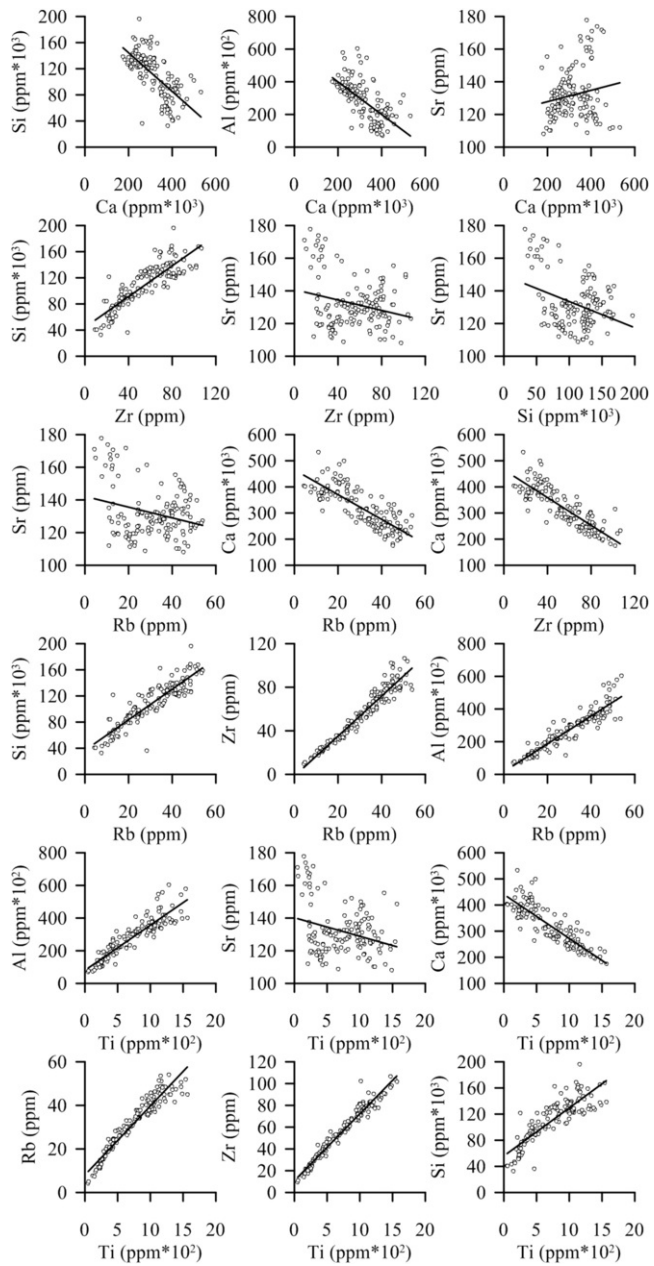


Fig. S1 Correlation plots between elements concentrations (XRF data converted to ppm).

alt-text: Fig. S1

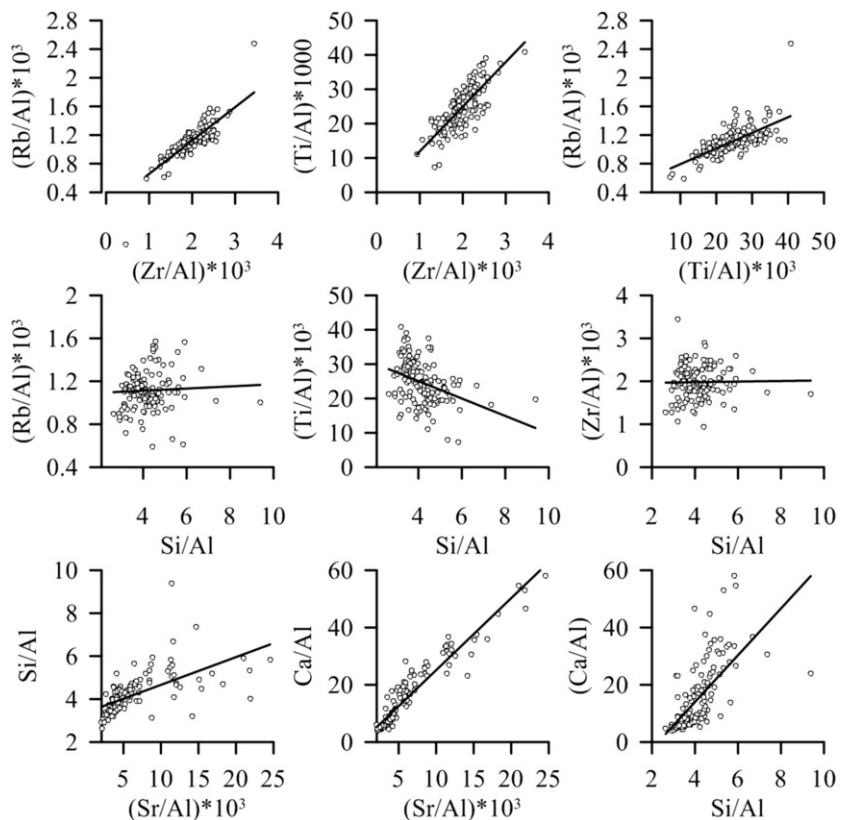


Fig. S2 Correlation plots between selected series of elements/Al ratios.

alt-text: Fig. S2

[Multimedia Component 1](#)

Table S1 Full analytical details for individual crystals of tephra POP4.

alt-text: Table S1

Highlights

- A multiproxy record from a lacustrine succession covering the MIS5 is presented.
- All proxies show a coherent picture of hydrological and environmental changes.
- The record highlights several dry events within the interglacial.
- Comparison with regional paleoclimate framework shows consistent features.

Queries and Answers

Query:

Please provide a definition for the significance of the boldfaced data in Table 1.

Answer: reported in bold the new $^{40}\text{Ar}/^{39}\text{Ar}$ for X6 layer.

Query:

Your article is registered as a regular item and is being processed for inclusion in a regular issue of the journal. If this is NOT correct and your article belongs to a Special Issue/Collection please contact k.kunchala@elsevier.com immediately prior to returning your corrections.

Answer: The article is a regular item

Query:

The author names have been tagged as given names and surnames (surnames are highlighted in teal color). Please confirm if they have been identified correctly.

Answer: all authors names have been correctly identified

Query:

The citation "Zanchetta et al., 2016" has been changed to "Zanchetta et al., 2016a, b" to match the author name/date in the reference list. Please check if the change is fine in this occurrence and modify the subsequent occurrences, if necessary.

Answer: Zanchetta 2016a is from Biogeoscience, Zanchetta 2016b is from AMQ, it has been corrected throughout the text and in the references list

Query:

Citation "Petrosino et al., 2014" has not been found in the reference list. Please supply full details for this reference.

Answer:

Petrosino, P., Jicha, B. R., Mazzeo, F. C., & Ermolli, E. R. (2014). A high resolution tepochronological record of MIS 14-12 in the Southern Apennines (Acerno Basin, Italy). *Journal of Volcanology and Geothermal Research*, 274, 34-50.

Query:

The citation "Gemelli et al. (2014)" has been changed to "Gemelli et al. (2015)" to match the author name/date in the reference list. Please check if the change is fine in this occurrence and modify the subsequent occurrences, if necessary.

Answer: the citation is now correct

Query:

Citation "Steiger and Jäger (1977)" has not been found in the reference list. Please supply full details for this reference.

Answer: Steiger, R.H., Jäger, E., 1977. Subcommission on geochronology: convention on the use of decay constants in geo- and cosmochronology. *Earth Planet. Sci. Lett.* 36, 359-362.

Query:

Please confirm whether the data " $J = 3.515 \cdot 10^{-4} \pm 1.410 \cdot 10^{-6}$ " should be changed to " $J = 3.515 \cdot 10^{-4} \pm 1.410 \cdot 10^{-6}$ ".

Answer: yes, please change

Query:

Citation "Lee et al., 2006" has not been found in the reference list. Please supply full details for this reference.

Answer: Lee, J.Y., Marti, K., Severinghaus, J.P., Kawamura, K., Yoo, H.-S., Lee, J.B., Kim, J.S.,

2006. A redetermination of the isotopic abundances of atmospheric Ar. *Geochim.*

Cosmochim. Acta 70, 4507e4512.

Query:

Citation "Kuiper et al., 2008" has not been found in the reference list. Please supply full details for this reference.

Answer: please remove this reference

Query:

Citation "Renne et al., 2011" has not been found in the reference list. Please supply full details for this reference.

Answer:

Renne, P. R., Balco, G., Ludwig, K. R., Mundil, R., & Min, K. (2011). Response to the comment by WH Schwarz et al. on "Joint determination of 40 K decay constants and 40 Ar*/40 K for the Fish Canyon sanidine standard, and improved accuracy for 40 Ar/39 Ar geochronology" by PR Renne et al.(2010). *Geochimica et Cosmochimica Acta*, 75(17), 5097-5100.

Query:

Citation "Jicha et al., 2016" has not been found in the reference list. Please supply full details for this reference.

Answer:

Jicha, B. R., Singer, B. S., & Sobol, P. (2016). Re-evaluation of the ages of 40 Ar/39 Ar sanidine standards and supereruptions in the western US using a Noblesse multi-collector mass spectrometer. *Chemical Geology*, 431, 54-66.

Query:

Please confirm whether the data " $2.0\text{-}2.2 \cdot 10^{-17}$ and $5.0\text{-}6.0 \cdot 10^{-19}\text{mol}$ " should be changed to " $2.0\text{-}2.2 \cdot 10^{-17}$ and $5.0\text{-}6.0 \cdot 10^{-19}\text{mol}$ ".

Answer: yes, right

Query:

The citation "Methods" has been changed to "Materials and methods" to match the section provided in the article. Please check if this change is appropriate, and amend if necessary.

Answer: right

Query:

The citation "Giaccio et al., 2015" has been changed to "Giaccio et al., 2015a, b" to match the author name/date in the reference list. Please check if the change is fine in this occurrence and modify the subsequent occurrences, if necessary.

Answer: Giaccio et al., 2015a is from Gology, Giaccio et al., 2015b is from scientific Drilling. Citantions in the text and in the references list are ok.

Query:

All occurrences of the unit “% wt” have been changed to “wt%” for clarity and consistency. Please check if this change is appropriate, and amend if necessary.

Answer: right

Query:

Citation "NGRIP members, 2004" has not been found in the reference list. Please supply full details for this reference.

Answer: North Greenland Ice Core Project Members. 2004. High-resolution record of Northern Hemisphere climate extending into the last interglacial period. Nature 431: 147-151.

Query:

Citation "McManus et al., 2004" has not been found in the reference list. Please supply full details for this reference.

Answer: McManus JF, Bond GC, Broecker WS, et al. 1994. High-resolution climate records from the North Atlantic during the Last Interglacial. Nature 371: 326-329.

Query:

The citation “Boch et al., 2008” has been changed to “Boch et al., 2011” to match the author name/date in the reference list. Please check if the change is fine in this occurrence and modify the subsequent occurrences, if necessary.

Answer: Boch et al., 2011 is the corrected one

Query:

The citation “Section 4.2.1” has been changed to “Section 4.2” since only Section 4.2 has been provided in the article. Please check if this change is appropriate, and amend if necessary.

Answer: right

Query:

Table 3 is not cited in the text. Please check that the citation suggested by the copyeditor is in the appropriate place, and correct if necessary.

Answer: Citation of Table 3 has been addedd in the right position, please remove it from here.

Query:

D’Addabbo et al., 2015 was mentioned here but not in the reference list, however D’Addabbo et al. was included in the list but was uncited in the text. No similar reference was given therefore it was presumed that D’Addabbo et al., 2015 should be linked to the reference found in the list. Please check if appropriate.

Answer: D'Addabbo et al., 2015 is the right citation, here and in the reference list

Query:

Citation "Sánchez-Goñi et al., 2007" has not been found in the reference list. Please supply full details for this reference.

Answer: Sánchez Goñi MF. 2007. Introduction to climate and vegetation in Europe during MIS5. *Developments in Quaternary Sciences* 7: 197-205.

Query:

Citation "Sánchez-Goñi et al., 2005" has not been found in the reference list. Please supply full details for this reference.

Answer: it has to be changed to 2007

Query:

The citation "Bauch et al., 2011" has been changed to "Bauch et al., 2012" to match the author name/date in the reference list. Please check if the change is fine in this occurrence and modify the subsequent occurrences, if necessary.

Answer: Bauch et al., 2012 is the corrected one

Query:

Citation "Mokeddem et al., 2014" has not been found in the reference list. Please supply full details for this reference.

Answer:

Mokeddem, Z., McManus, J. F., & Oppo, D. W. (2014). Oceanographic dynamics and the end of the last interglacial in the subpolar North Atlantic. *Proceedings of the National Academy of Sciences*, 111(31), 11263-11268.

Query:

Uncited references: This section comprises references that occur in the reference list but not in the body of the text. Please position each reference in the text or, alternatively, delete it. Thank you.

Answer: NGRIP reference is the only one that have to be inserted

Query:

One sponsor name has been edited to a standard format that enables better searching and identification of your article. Please check and correct if necessary.

Answer: right